Eur. J. Stat. 6 (2026) 16
doi: 10.28924/ada/stat.6.16

Transmission Dynamics and Optimal Control of Malaria-Dengue Co-infection: A Cost-Effectiveness Analysis

Francis Agono[1,3], Godwin Onuche Acheneje[1,3], Benedict Celestine Agbata[2], A.K. Awasthi[4], Hambeer Singh[5], Aseel Smerat[6,7], M. Manivel[8,*], Bolarinwa Bolaji[1,3]

[1] *Department of Mathematical Sciences, Prince Abubakar Audu University, Anyigba, Kogi State, Nigeria*
[2] *Department of Mathematics and Statistics, Faculty of Science, Confluence University of Science and Technology, Osara, Nigeria*
[3] *Laboratory of Mathematical Epidemiology, Prince Abubakar Audu University, Anyigba, Kogi State, Nigeria*
[4] *Department of Mathematics, School of Chemical Engineering and Physical Sciences, Lovely Professional University, Phagwara, Punjab, India*
[5] *Department of Mathematics, Rawal Institute of Engineering & Technology, Faridabad, India*
[6] *Faculty of Educational Sciences, Al-Ahliyya Amman University, Amman 19328, Jordan*
[7] *Centre for Research Impact & Outcome, Chitkara University Institute of Engineering and Technology, Chitkara University, Rajpura 140401, Punjab, India*
[8] *Department of Mathematics, Vel Tech Rangarajan Dr. Sagunthala R&D Institute of Science and Technology, Chennai 600062, India*
[*] *Correspondence: manivelmani718@gmail.com*

Abstract. This study presents a comprehensive deterministic compartmental model for malaria-dengue co-infection incorporating distinct vector populations (*Anopheles* for malaria and *Aedes* for dengue), disease-specific progression pathways, and co-infection compartments. The model is rigorously analyzed to establish positivity, boundedness, disease-free and endemic equilibria, and basic reproduction numbers. Optimal control theory is applied to evaluate six time-dependent intervention strategies: insecticide-treated bed nets (ITNs), indoor residual spraying (IRS), environmental management, personal protection measures, treatment compliance, and vaccination. Model parameters are estimated using Brazilian malaria and dengue case data (2011-2023). Sensitivity analysis identifies key parameters influencing disease transmission. Cost-effectiveness analysis using infection averted ratio (IAR), average cost-effectiveness ratio (ACER), and incremental cost-effectiveness ratio (ICER) reveals that the combined implementation of all six control measures (Strategy 9) is most cost-effective, averting 9,200 infections (35.38% reduction) at an ACER of 3,756.536. These findings provide crucial guidance for designing economically efficient intervention strategies in resource-constrained co-endemic settings.

Received: 5 May 2026.
Key words and phrases. malaria; dengue fever; co-infection; optimal control; cost benefit analysis.

1. Introduction

Malaria remains one of the most devastating infectious diseases globally, with an estimated 249 million cases and 608,000 deaths reported in 2022, predominantly affecting sub-Saharan Africa where children under five years account for approximately 80% of malaria-related mortality [1]. The disease is caused by *Plasmodium* parasites transmitted through the bites of infected female *Anopheles* mosquitoes, with *Plasmodium falciparum* being the most lethal species. Clinical manifestations include fever, chills, headache, and in severe cases, cerebral malaria, severe anemia, and multi-organ failure. Despite significant progress in malaria control through insecticide-treated bed nets, indoor residual spraying, and artemisinin-based combination therapies, the disease continues to impose substantial morbidity and mortality in endemic regions [2].

Dengue fever, caused by any of four serotypes of the dengue virus (DENV-1 to DENV-4), represents another major vector-borne disease of global public health concern. The World Health Organization estimates that approximately 3.9 billion people in over 129 countries are at risk of dengue infection, with an estimated 390 million infections occurring annually worldwide [3]. Transmitted primarily by *Aedes aegypti* and *Aedes albopictus* mosquitoes, dengue manifests clinically as a spectrum ranging from asymptomatic or mild febrile illness to severe dengue characterized by plasma leakage, hemorrhagic manifestations, and organ impairment. The absence of specific antiviral treatment and the limited availability of vaccines underscore the critical importance of vector control and early clinical management in reducing dengue-associated morbidity and mortality [4].

The geographic overlap between malaria-endemic regions and dengue-endemic areas, particularly in tropical and subtropical regions of Africa, Southeast Asia, and the Americas, creates conditions favorable for co-infection [5]. Both diseases share similar initial clinical presentations—fever, headache, myalgia, and thrombocytopenia—making accurate differential diagnosis challenging in resource-limited settings where laboratory confirmation is often unavailable [6]. Studies have documented simultaneous malaria-dengue co-infections in various endemic countries, with prevalence rates varying from 0.8% to 6.5% among febrile patients depending on local transmission intensities [7]. Co-infected patients often experience more severe clinical outcomes, including higher rates of thrombocytopenia, hepatic dysfunction, and complications requiring hospitalization compared to those with single infections [6]. The overlapping symptomatology and concurrent circulation of both pathogens pose significant diagnostic and therapeutic challenges, potentially leading to delayed treatment, inappropriate antimalarial use in dengue cases, or missed dengue diagnosis in malaria-endemic regions [8].

Mathematical modeling has emerged as an indispensable tool for understanding infectious disease dynamics and evaluating intervention strategies [9,10]. Compartmental models, particularly those based on susceptible-exposed-infected-recovered (SEIR) frameworks, have successfully elucidated transmission patterns and guided public health responses for numerous vector-borne diseases. Anderson and May [11] established foundational principles for modeling vector-borne

disease transmission incorporating mosquito population dynamics and human-vector contact patterns. For malaria specifically, Ross-Macdonald models and their extensions have characterized transmission thresholds, vectorial capacity, and the impact of control interventions on disease persistence [12]. Similarly, dengue transmission models have incorporated multiple serotypes, antibody-dependent enhancement, and temperature-dependent mosquito dynamics to predict outbreak patterns and assess intervention strategies [13].

Optimal control theory, grounded in Pontryagin's maximum principle, provides a rigorous mathematical framework for determining intervention strategies that minimize disease burden while accounting for implementation costs [14]. Researchers have successfully applied optimal control to various vector-borne disease models. For malaria, studies have identified optimal combinations of vector control, treatment, and prevention measures that maximize population health benefits within budget constraints [15,16]. In dengue control, optimal control frameworks have guided integrated vector management strategies, including larviciding, adulticiding, and community-based environmental interventions [17]. Cost-benefit analyses complement these approaches by quantifying the economic efficiency of different intervention scenarios, enabling policymakers to prioritize strategies with the most favorable benefit-cost ratios in resource-constrained endemic settings.

Recent advances in co-infection modeling have addressed multiple concurrent vector-borne diseases. Omame et al. [18] investigated dengue, chikungunya, and Zika co-circulation using mathematical frameworks with time-dependent controls, demonstrating complex interplay between co-circulating arboviruses. Tchoumi et al. [19] developed mathematical models for malaria and COVID-19 co-infection, incorporating optimal control strategies for dual disease management. Mekonen et al. [20] formulated models examining infectious disease co-infection dynamics with control interventions. However, despite documented clinical evidence of malaria-dengue co-infections and their public health significance, comprehensive mathematical models explicitly incorporating both *Anopheles* and *Aedes* vector populations, disease-specific progression pathways, co-infection compartments, and multiple optimal control strategies remain notably scarce in the literature.

While several studies have examined malaria and dengue individually or in simplified co-infection frameworks, significant gaps persist in modeling the complete spectrum of disease interactions with comprehensive control strategies. Existing models often overlook critical features such as distinct vector populations with separate transmission cycles, explicit co-exposed and co-infected compartments accounting for altered disease progression and severity in co-infection, treatment compartments for single and dual infections, or the synergistic effects of simultaneous vector control and treatment interventions targeting both diseases. Furthermore, few studies have conducted rigorous cost-benefit analyses comparing multiple control combinations to identify economically optimal strategies for resource-constrained settings where both malaria and dengue are co-endemic.

This study addresses these gaps by developing a comprehensive deterministic compartmental model for malaria-dengue co-infection that explicitly incorporates separate vector populations (*Anopheles* for malaria and *Aedes* for dengue), disease-specific exposed, infected, treated, and recovered classes, as well as co-exposed, co-infected, and co-treatment compartments. We rigorously analyze the model's mathematical properties, including positivity and boundedness of solutions, existence and stability of disease-free and endemic equilibria, and derive the basic reproduction numbers for malaria, dengue, and co-infection scenarios. Subsequently, we formulate and solve an optimal control problem incorporating time-dependent vector control strategies (insecticide-treated bed nets and indoor residual spraying for malaria vectors, environmental management and adulticiding for dengue vectors) and treatment interventions for both single infections and co-infections. Through numerical simulations calibrated with parameter estimates from endemic regions and comprehensive cost-benefit analysis, we identify economically efficient intervention combinations that minimize disease burden while optimizing resource allocation in co-endemic settings.

The remainder of this manuscript is structured as follows: Section 2 presents the model formulation, parameter descriptions, underlying assumptions, and data fitting methodology. Section 4 develops the optimal control framework, derives necessary conditions using Pontryagin's maximum principle, and establishes the optimality system. Section 4.2 presents numerical simulations illustrating intervention impacts, sensitivity analyses, and cost-benefit comparisons. Section 5 provides concluding remarks, policy recommendations, and directions for future research.

2. Model Formulation

The assumptions used in the formulation of the model are:

(1) Homogeneous mixing is assumed within the human population, meaning that every individual has an equal probability of contact with any other individual, facilitating random transmission of both malaria and dengue via their respective mosquito vectors. [11]
(2) Both malaria and dengue are vector-borne diseases, transmitted by separate mosquito populations (Anopheles mosquitoes for malaria and Aedes mosquitoes for dengue), with infected vectors contributing to the force of infection, and humans recovering from each disease with temporary immunity. [21]
(3) Co-infection with malaria and dengue increases disease severity and may alter progression rates, necessitating separate compartments for co-exposed and co-infected individuals. [22]
(4) Treatment is available for both diseases and is incorporated into the model, reducing infectivity and disease-induced mortality, though efficacy may be reduced in co-infected cases.

A deterministic compartmental model for the transmission dynamics of malaria–dengue co-infection is proposed. The model divides the human population into susceptible individuals, those exposed or infected with malaria only, those exposed or infected with dengue only, and those co-infected with both diseases. Separate vector (mosquito) populations are included to account for the distinct transmission cycles of malaria and dengue.

The total human population at time t is denoted by $N_h(t)$ and is subdivided into the following compartments: Susceptible humans $S_h(t)$, Exposed to malaria only $E_m(t)$, Infected with malaria only $I_m(t)$, Treated for malaria only $T_m(t)$, Recovered from malaria only $R_m(t)$, Exposed to dengue only $E_d(t)$, Infected with dengue only $I_d(t)$, Treated for dengue only $T_d(t)$, Recovered from dengue only $R_d(t)$, Exposed to both diseases $E_{md}(t)$, Infected with both diseases $I_{md}(t)$, and Treated for co-infection $T_{md}(t)$. The malaria vector population is divided into Susceptible malaria vectors $S_{vm}(t)$ and Infected malaria vectors $I_{vm}(t)$. The dengue vector population is divided into Susceptible dengue vectors $S_{vd}(t)$ and Infected dengue vectors $I_{vd}(t)$.

Recruitment into the susceptible human population occurs at rate Λ_h. Natural death rate is μ_h in all human compartments. No vaccination is considered in this formulation.

The force of infection for malaria is:

$$\lambda_m = \frac{b_m \beta_m I_{vm}}{N_h},$$

where b_m is the biting rate of Anopheles mosquitoes, β_m is the transmission probability from infected malaria vector to human, and I_{vm} is the number of infected malaria vectors.

The force of infection for dengue is:

$$\lambda_d = \frac{b_d \beta_d I_{vd}}{N_h},$$

where b_d, β_d are the corresponding parameters for Aedes mosquitoes and dengue transmission. Susceptible individuals become exposed to malaria at rate $\lambda_m S_h$ or to dengue at rate $\lambda_d S_h$. Co-infection occurs when individuals in malaria-only classes acquire dengue (or vice versa) at modified rates, leading to co-exposed and co-infected compartments.

Exposed malaria individuals progress to infected at rate θ_1; infected malaria individuals acquire dengue at rate θ_4 or receive treatment at rate α_1. Similar progression and treatment rates apply to dengue-only classes. Co-infected individuals have modified progression, treatment, and mortality rates.

Malaria vectors are recruited at rate Λ_{vm}, die naturally at rate μ_v, and become infected at rate $\lambda_{vm} S_{vm}$, where

$$\lambda_{vm} = \frac{b_m \gamma_m (I_m + I_{md})}{N_h}$$

and γ_m is the transmission probability from infectious humans to malaria vectors. Analogous equations hold for dengue vectors with parameters b_d, γ_d, Λ_{vd}, and λ_{vd}.

The total human population is

$$N_h(t) = S_h + E_m + I_m + T_m + R_m + E_d + I_d + T_d + R_d + E_{md} + I_{md} + T_{md}.$$

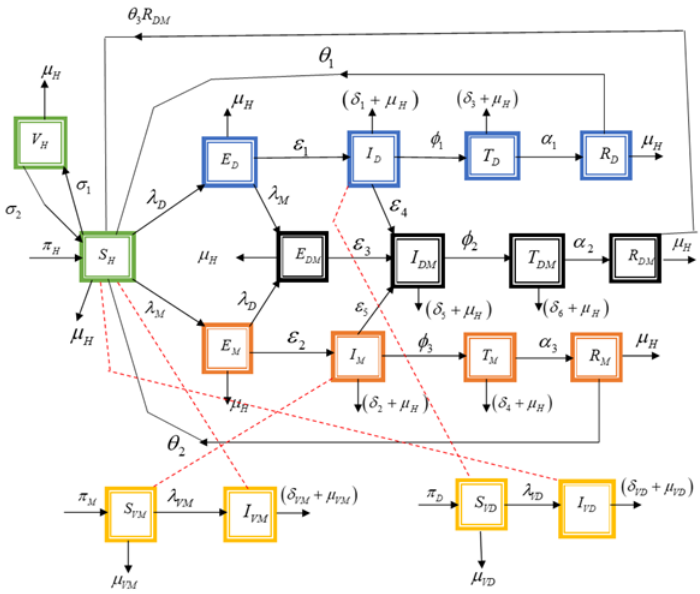

FIGURE 1. **Schematic flow diagram of the malaria–dengue co-infection mathematical model.** The diagram illustrates parallel vector-borne transmission pathways for malaria (Anopheles vectors, blue) and dengue (Aedes vectors, red), with co-infection compartments (mixed). Forces of infection λ_m (malaria) and λ_d (dengue) drive transitions from susceptible S_h, with treatment classes T and recovery R. Natural and disease-induced deaths are included throughout.

2.1. **Model Equations.** The system of differential equations governing the co-infection dynamics is given in Equation (1), including the force of infection terms defined above.

$$
\begin{aligned}
\frac{dS_h}{dt} &= \Lambda_h - \lambda_m S_h - \lambda_d S_h - \mu_h S_h, \\
\frac{dE_m}{dt} &= \lambda_m S_h - \lambda_d E_m - (\theta_1 + \mu_h) E_m, \\
\frac{dI_m}{dt} &= \theta_1 E_m - (\theta_4 + \alpha_1 + \delta_1 + \mu_h) I_m, \\
\frac{dT_m}{dt} &= \alpha_1 I_m - (\phi_1 + \delta_6 + \mu_h) T_m, \\
\frac{dR_m}{dt} &= \phi_1 T_m + \phi_2 T_{md} - (\varepsilon + \mu_h) R_m, \\
\frac{dE_d}{dt} &= \lambda_d S_h - \lambda_m E_d - (\theta_3 + \mu_h) E_d, \\
\frac{dI_d}{dt} &= \theta_3 E_d - (\theta_5 + \alpha_2 + \delta_2 + \mu_h) I_d, \\
\frac{dT_d}{dt} &= \alpha_2 I_d - (\phi_3 + \delta_7 + \mu_h) T_d, \\
\frac{dR_d}{dt} &= \phi_3 T_d + \phi_4 T_{md} - (\varepsilon + \mu_h) R_d,
\end{aligned}
\tag{1}
$$

$$\frac{dE_{md}}{dt} = \lambda_m E_d + \lambda_d E_m - (\theta_2 + \mu_h)E_{md},$$
$$\frac{dI_{md}}{dt} = \theta_2 E_{md} + \theta_4 I_m + \theta_5 I_d - (\alpha_3 + \delta_3 + \mu_h)I_{md},$$
$$\frac{dT_{md}}{dt} = \alpha_3 I_{md} - (\phi_2 + \phi_4 + \delta_8 + \mu_h)T_{md},$$
$$\frac{dS_{vm}}{dt} = \Lambda_{vm} - \lambda_{vm} S_{vm} - \mu_v S_{vm},$$
$$\frac{dI_{vm}}{dt} = \lambda_{vm} S_{vm} - (\mu_v + \delta_{vm})I_{vm},$$
$$\frac{dS_{vd}}{dt} = \Lambda_{vd} - \lambda_{vd} S_{vd} - \mu_v S_{vd},$$
$$\frac{dI_{vd}}{dt} = \lambda_{vd} S_{vd} - (\mu_v + \delta_{vd})I_{vd},$$

where the forces of infection are defined as:

$$\lambda_m = \frac{b_m \beta_m I_{vm}}{N_h}, \quad \lambda_d = \frac{b_d \beta_d I_{vd}}{N_h},$$
$$\lambda_{vm} = \frac{b_m \gamma_m (I_m + I_{md})}{N_h}, \quad \lambda_{vd} = \frac{b_d \gamma_d (I_d + I_{md})}{N_h}.$$

TABLE 1. **Description of Model Parameters**

Parameter	**Detailed Description**
Λ_h	Recruitment rate into the susceptible human population.
Λ_{vm}	Recruitment rate into the susceptible malaria vector population.
Λ_{vd}	Recruitment rate into the susceptible dengue vector population.
μ_h	Natural death rate in humans.
μ_v	Natural death rate in vectors.
θ_1	Progression rate from malaria-exposed only (E_m) to malaria-infected only (I_m).
θ_2	Progression rate from co-exposed (E_{md}) to co-infected (I_{md}).
θ_3	Progression rate from dengue-exposed only (E_d) to dengue-infected only (I_d).
θ_4	Rate at which malaria-infected only (I_m) acquire dengue (move to I_{md}).
θ_5	Rate at which dengue-infected only (I_d) acquire malaria (move to I_{md}).
α_1	Treatment initiation rate for malaria-only infected (I_m).

Continued on next page

Table 1 – continued from previous page

Parameter	Detailed Description
α_2	Treatment initiation rate for dengue-only infected (I_d).
α_3	Treatment initiation rate for co-infected individuals (I_{md}).
ϕ_1	Recovery rate from malaria treatment only (T_m).
ϕ_3	Recovery rate from dengue treatment only (T_d).
ϕ_2, ϕ_4	Recovery rates from co-infection treatment (T_{md}) contributing to malaria and dengue recovered classes, respectively.
δ_1	Malaria-induced death rate in malaria-infected only (I_m).
δ_2	Dengue-induced death rate in dengue-infected only (I_d).
δ_3	Disease-induced death rate in co-infected (I_{md}).
$\delta_6, \delta_7, \delta_8$	Disease-induced death rates in treated classes.
ε	Loss of immunity rate (assumed same for malaria and dengue recovered).
b_m, b_d	Biting rates of malaria and dengue vectors, respectively.
β_m, β_d	Transmission probabilities from infected vectors to humans.
γ_m, γ_d	Transmission probabilities from infectious humans to vectors.
δ_{vm}, δ_{vd}	Disease induced death rate of malaria and dengue fever vectors

TABLE 2. **Description of model variables**

Variable	Description
$S_h(t)$	Susceptible humans
$E_m(t)$	Exposed to malaria only
$I_m(t)$	Infected with malaria only
$T_m(t)$	Treated for malaria only
$R_m(t)$	Recovered from malaria only
$E_d(t)$	Exposed to dengue only
$I_d(t)$	Infected with dengue only
$T_d(t)$	Treated for dengue only
$R_d(t)$	Recovered from dengue only
$E_{md}(t)$	Exposed to both diseases
$I_{md}(t)$	Infected with both diseases
$T_{md}(t)$	Treated for co-infection
$S_{vm}(t)$	Susceptible malaria vectors
$I_{vm}(t)$	Infected malaria vectors
$S_{vd}(t)$	Susceptible dengue vectors
$I_{vd}(t)$	Infected dengue vectors
$N_h(t)$	Total human population

3. Analysis of the Malaria–Dengue Co-infection Model

3.1. Invariant Region of the Model.

Theorem 1. *The solutions of the malaria–dengue co-infection model are feasible for all $t > 0$ if they enter the invariant region $\Omega = \Omega_H \times \Omega_{V_M} \times \Omega_{V_D} \subset \mathbb{R}^{14}_+ \times \mathbb{R}^2_+ \times \mathbb{R}^2_+$.*

Proof. We prove that all feasible solutions are uniformly bounded in the biologically meaningful region $\Omega_H \subset \mathbb{R}^{14}_+$ (human population), $\Omega_{V_M} \subset \mathbb{R}^2_+$ (malaria mosquito population), and $\Omega_{V_D} \subset \mathbb{R}^2_+$ (dengue mosquito population).

Define the sets:

$$\Omega_H = \Big\{(S_H, E_D, E_M, E_{DM}, I_D, I_M, I_{DM}, T_D, T_M, T_{DM}, V_H, R_D, R_M, R_{DM}) \in \mathbb{R}^{14}_+ : N_H(t) \le \frac{\pi_H}{\mu_H}\Big\},$$

$$\Omega_{V_M} = \{(S_{VM}, I_{VM}) \in \mathbb{R}^2_+ : N_{VM}(t) \le \frac{\pi_M}{\mu_{VM}}\},$$

$$\Omega_{V_D} = \{(S_{VD}, I_{VD}) \in \mathbb{R}^2_+ : N_{VD}(t) \le \frac{\pi_D}{\mu_{VD}}\},$$

where the total populations are

$$N_H(t) = S_H + E_D + E_M + E_{DM} + I_D + I_M + I_{DM} + T_D + T_M + T_{DM} + V_H + R_D + R_M + R_{DM},$$
$$N_{VM}(t) = S_{VM} + I_{VM}, \quad N_{VD}(t) = S_{VD} + I_{VD}.$$

Adding all the human compartment equations gives

$$\frac{dN_H}{dt} = \pi_H - \mu_H N_H - \delta_1 I_D - \delta_2 I_M - \delta_5 I_{DM} - \delta_3 T_D - \delta_4 T_M - \delta_6 T_{DM}.$$

Since all disease-induced death rates satisfy $\delta_i \ge 0$, it follows that

$$\frac{dN_H}{dt} \le \pi_H - \mu_H N_H.$$

Solving the linear differential inequality (standard comparison theorem / integrating factor) with initial condition $N_H(0) = N_{H0}$ yields

$$N_H(t) \le \frac{\pi_H}{\mu_H} + \left(N_{H0} - \frac{\pi_H}{\mu_H}\right) e^{-\mu_H t}.$$

As $t \to \infty$, the exponential term vanishes, so

$$N_H(t) \le \frac{\pi_H}{\mu_H} \quad \text{for sufficiently large } t,$$

and clearly $N_H(t) \ge 0$ (non-negative recruitment and non-negative outflows). Thus Ω_H is positively invariant.

For the malaria vector population:

$$\frac{dN_{VM}}{dt} = \pi_M - \mu_{VM} S_{VM} - (\delta_{VM} + \mu_{VM}) I_{VM} \leq \pi_M - \mu_{VM} N_{VM}.$$

By the same reasoning,

$$0 \leq N_{VM}(t) \leq \frac{\pi_M}{\mu_{VM}} \quad \Rightarrow \quad \Omega_{V_M} \text{ is positively invariant.}$$

Likewise for the dengue vector population:

$$\frac{dN_{VD}}{dt} = \pi_D - \mu_{VD} S_{VD} - (\delta_{VD} + \mu_{VD}) I_{VD} \leq \pi_D - \mu_{VD} N_{VD},$$

so

$$0 \leq N_{VD}(t) \leq \frac{\pi_D}{\mu_{VD}} \quad \Rightarrow \quad \Omega_{V_D} \text{ is positively invariant.}$$

Therefore the product region $\Omega = \Omega_H \times \Omega_{V_M} \times \Omega_{V_D}$ is positively invariant for the full system.

□

3.2. **Positivity of Solutions of the Model.**

Theorem 2. *Let the initial conditions be non-negative:* $S_H(0), E_D(0), E_M(0), E_{DM}(0), I_D(0), I_M(0), I_{DM}(0), T_D(0), T_M(0), T_{DM}(0), V_H(0), R_D(0), R_M(0), R_{DM}(0), S_{VM}(0), I_{VM}(0), S_{VD}(0), I_{VD}(0) \geq 0$. *Then every solution of the model remains non-negative for all* $t > 0$.

Proof. We prove by contradiction and standard differential inequality arguments that no compartment can become negative in finite time.

Suppose there exists a first time $t^* > 0$ such that at least one compartment reaches zero while others are still non-negative, and some become negative immediately after. We show this leads to a contradiction.

For S_H:

$$\frac{dS_H}{dt} = \pi_H + \theta_1 R_D + \theta_2 R_M + \sigma_2 V_H - (\lambda_D + \lambda_M + \sigma_1 + \mu_H) S_H \geq -(\lambda_D + \lambda_M + \sigma_1 + \mu_H) S_H.$$

Thus

$$S_H(t) \geq S_H(0) \exp\left(- \int_0^t (\lambda_D(s) + \lambda_M(s) + \sigma_1 + \mu_H)\, ds \right) \geq 0.$$

For V_H:

$$\frac{dV_H}{dt} = \sigma_1 S_H - (\sigma_2 + \mu_H) V_H \geq -(\sigma_2 + \mu_H) V_H \quad \Rightarrow \quad V_H(t) \geq V_H(0) e^{-(\sigma_2 + \mu_H)t} \geq 0.$$

For E_D:

$$\frac{dE_D}{dt} = \lambda_D S_H - (\lambda_M + \varepsilon_1 + \mu_H) E_D \geq -(\lambda_M + \varepsilon_1 + \mu_H) E_D,$$

so $E_D(t) \geq 0$ by the same exponential bound.

- Similarly for E_M:

$$\frac{dE_M}{dt} \geq -(\lambda_D + \varepsilon_2 + \mu_H) E_M \quad \Rightarrow \quad E_M(t) \geq 0.$$

For E_{DM}:

$$\frac{dE_{DM}}{dt} = \lambda_M E_D + \lambda_D E_M - (\varepsilon_3 + \mu_H)E_{DM} \geq -(\varepsilon_3 + \mu_H)E_{DM} \quad \Rightarrow \quad E_{DM}(t) \geq 0.$$

- For the infectious classes I_D, I_M, I_{DM} the pattern continues:

$$\frac{dI_D}{dt} = \varepsilon_1 E_D - (\phi_1 + \varepsilon_4 + \delta_1 + \mu_H)I_D \geq -(\phi_1 + \varepsilon_4 + \delta_1 + \mu_H)I_D,$$

and analogously for I_M and I_{DM}.

- The same linear lower bound holds for $T_D, T_M, T_{DM}, R_D, R_M, R_{DM}$.

- Finally, for the vectors:

$$\frac{dS_{VM}}{dt} = \pi_M - (\lambda_{VM} + \mu_{VM})S_{VM} \geq -(\lambda_{VM} + \mu_{VM})S_{VM},$$

$$\frac{dI_{VM}}{dt} = \lambda_{VM} S_{VM} - (\delta_{VM} + \mu_{VM})I_{VM} \geq -(\delta_{VM} + \mu_{VM})I_{VM},$$

and likewise for S_{VD} and I_{VD}.

Since each equation is of the form

$$\frac{dx}{dt} \geq -k(t)x + f(t), \quad k(t) \geq 0, \quad f(t) \geq 0 \quad \text{or} \quad f(t) = 0,$$

and the inflow terms are always non-negative whenever the source compartments are non-negative, no compartment can cross zero from above before t^*. By continuity and the fact that the right-hand side is locally Lipschitz in the positive orthant, the solution cannot become negative. Hence all compartments remain ≥ 0 for all $t > 0$. □

These two results together guarantee that the model is well-posed in the non-negative orthant and that solutions remain biologically meaningful (bounded and non-negative) for all time.

3.3. **Asymptotic stability of the Dengue disease free equilibrium of the model.** The stable condition in which there is no infection (or illness), a point where $E_D = I_D = T_D = R_D = S_{VD} = I_{VD} = 0$ is known as the disease-free equilibrium point (DFE), and it is given by:

$\varepsilon_0 = \{S^*, E_D^*, I_D^*, T_D^*, V^*, R_D^*, S_{VD}^*, I_{VD}^*\} = \left\{\frac{\pi_H(\mu_H+\sigma_2)}{\mu_H(\sigma_1+\mu_H+\sigma_2)}, 0, 0, 0, \frac{\pi_H\sigma_1}{\mu_H(\sigma_1+\mu_H+\sigma_2)}, 0, \frac{\pi_D}{\mu_{VD}}, 0\right\}$

Similarly, the disease free equilibrium point of the malaria only sub-model is given as

$\varepsilon_0 = \{S^*, E_M^*, I_M^*, T_M^*, V^*, R_M^*, S_{VM}^*, I_{VM}^*\} = \left\{\frac{\pi_H(\mu_H+\sigma_2)}{\mu_H(\sigma_1+\mu_H+\sigma_2)}, 0, 0, 0, \frac{\pi_H\sigma_1}{\mu_H(\sigma_1+\mu_H+\sigma_2)}, 0, \frac{\pi_M}{\mu_{VM}}, 0\right\}$

3.4. **Basic Reproduction Number of the Malaria - Dengue co-infection model.** The basic Dengue reproduction number, indicated by R_0 is the mean quantity of secondary infections caused by a single malarial infected person placed into a completely susceptible community during the course of that person's infectious period. We use the next generation operator technique on the dynamical system (1) to get the reproduction number of the disease. where the new infection terms is given by matrix F while the remaining transfer terms in the model is given by matrix V as follows:

$$F_D = \begin{bmatrix} 0 & 0 & 0 & \frac{b\beta_D A_1}{A_2} \\ 0 & 0 & 0 & 0 \\ 0 & 0 & 0 & 0 \\ 0 & \frac{\beta_{VD}\pi_D\mu_H}{\mu_{VD}\pi_H} & 0 & 0 \end{bmatrix} \text{ and } V_D = \begin{bmatrix} A_3 & 0 & 0 & 0 \\ -\varepsilon_1 & A_4 & 0 & 0 \\ 0 & -\phi_1 & A_5 & 0 \\ 0 & 0 & 0 & A_6 \end{bmatrix}$$

$$F_D.{V_D}^{-1} = \begin{bmatrix} 0 & 0 & 0 & \frac{b\beta_D A_1}{A_2 A_6} \\ 0 & 0 & 0 & 0 \\ 0 & 0 & 0 & 0 \\ \frac{\beta_{VD}\pi_D\mu_H\varepsilon_3}{\mu_{VD}\pi_H A_3 A_4} & \frac{\beta_{VD}\pi_D\mu_H}{\mu_{VD}\pi_H A_4} & 0 & 0 \end{bmatrix}$$

Therefore, the basic reproduction number is given by:

$R_0^D = \rho\left(FV^{-1}\right)$

Where $\rho$is the dominant eigenvalue of FV^{-1}

As a result, the Dengue model's basic reproduction number is given by:

$R_0^D = \frac{\sqrt{\mu_{VD}\pi_H A_3 A_4 A_2 A_6 \beta_{VD}\pi_D\mu_H\varepsilon_3 b\beta_D A_1}}{\mu_{VD}\pi_H A_3 A_4 A_2 A_6}$

Where,

$A_1 = (\mu_H + \sigma_2), A_2 = (\sigma_1 + \mu_H + \sigma_2), A_3 = (\varepsilon_1 + \mu_H), A_4 = (\phi_1 + \delta_1 + \mu_H), A_5 = (\alpha_1 + \delta_3 + \mu_H)$, $A_6 = (\delta_{VD} + \mu_{VD})$.

Using similar technique, the basic reproduction number of the malaria only sub-model is computed thus:

$$F_M = \begin{bmatrix} 0 & 0 & 0 & \frac{b\beta_D B_1}{A_2} \\ 0 & 0 & 0 & 0 \\ 0 & 0 & 0 & 0 \\ 0 & \frac{\beta_{VM}\pi_M\mu_H}{\mu_{VM}\pi_H} & 0 & 0 \end{bmatrix} \text{ and } V_M = \begin{bmatrix} B_3 & 0 & 0 & 0 \\ -\varepsilon_2 & B_4 & 0 & 0 \\ 0 & -\phi_3 & B_5 & 0 \\ 0 & 0 & 0 & B_6 \end{bmatrix}$$

$$F_M.{V_M}^{-1} = \begin{bmatrix} 0 & 0 & 0 & \frac{b\beta_M B_1}{B_2 B_6} \\ 0 & 0 & 0 & 0 \\ 0 & 0 & 0 & 0 \\ \frac{\beta_{VM}\pi_M\mu_H\varepsilon_2}{\mu_{VM}\pi_H B_3 B_4} & \frac{\beta_{VM}\pi_M\mu_H}{\mu_{VM}\pi_H B_4} & 0 & 0 \end{bmatrix}$$

Therefore, the basic reproduction number is given by:

Where $\rho$is the dominant eigenvalue of FV^{-1}

As a result, the Malaria model's basic reproduction number is given by:

$R_0^M = \frac{\sqrt{\mu_{VM}\pi_H B_3 B_4 B_2 B_6 \beta_{VM}\pi_m\mu_H\varepsilon_2 b\beta_m B_1}}{\mu_{VM}\pi_H B_3 B_4 B_2 B_6}$

Where,

$B_1 = (\mu_H + \sigma_2), B_2 = (\sigma_1 + \mu_H + \sigma_2), B_3 = (\varepsilon_2 + \mu_H), B_4 = (\phi_3 + \delta_2 + \mu_H),$

$$B_5 = (\alpha_3 + \delta_4 + \mu_H)B_6 = (\delta_{VM} + \mu_{VM})\,.$$

The maximal reproduction number of both diseases is considered the basic reproduction in the context of the co-infection paradigm between HIV and Malaria.

$$R_0^{MH} = \max\left(R_0^D, R_0^M\right).$$

Where,

$$R_0^{DM} = \max\left(\frac{\sqrt{\mu_{VD}\pi_H A_3 A_4 A_2 A_6 \beta_{VD}\pi_D \mu_H \varepsilon_3 b\beta_D A_1}}{\mu_{VD}\pi_H A_3 A_4 A_2 A_6}, \frac{\sqrt{\mu_{VM}\pi_H B_3 B_4 B_2 B_6 \beta_{VM}\pi_m \mu_H \varepsilon_2 b\beta_m B_1}}{\mu_{VM}\pi_H B_3 B_4 B_2 B_6}\right)$$

$$R_0^{DM} = \begin{pmatrix} \frac{\sqrt{\mu_{VD}\pi_H\left(\varepsilon_1+\mu_H\right)\left(\phi_1+\delta_1+\mu_H\right)\left(\sigma_1+\mu_H+\sigma_2\right)\left(\delta_{VD}+\mu_{VD}\right)\beta_{VD}\pi_D\mu_H\varepsilon_3 b\beta_D\left(\mu_H+\sigma_2\right)}}{\mu_{VD}\pi_H\left(\varepsilon_1+\mu_H\right)\left(\phi_1+\delta_1+\mu_H\right)\left(\sigma_1+\mu_H+\sigma_2\right)\left(\delta_{VD}+\mu_{VD}\right)}, \\ \frac{\sqrt{\mu_{VM}\pi_H\left(\varepsilon_2+\mu_H\right)\left(\phi_3+\delta_2+\mu_H\right)\left(\sigma_1+\mu_H+\sigma_2\right)\left(\delta_{VM}+\mu_{VM}\right)\beta_{VM}\pi_m\mu_H\varepsilon_2 b\beta_m B_1}}{\mu_{VM}\pi_H\left(\varepsilon_2+\mu_H\right)\left(\phi_3+\delta_2+\mu_H\right)\left(\sigma_1+\mu_H+\sigma_2\right)\left(\delta_{VM}+\mu_{VM}\right)} \\ \end{pmatrix}$$

3.5. **Endemic equilibrium point of the Malaria - Dengue fever co-infection model.**

3.5.1. *Endemic Equilibrium of the Dengue Sub-model.*

Theorem 3. *When $R_0^H < 1$, the endemic equilibrium point is unstable, while for $R_0^H > 1$, it is locally asymptotically stable.*

Proof. We solve for each of the model's state variables and set all of the model's equations to zero to obtain the following:

$$S_H^{**} = -\frac{\pi_H A_3 A_4 A_5 A_8 A_9}{A_5 A_9 A_4((-\lambda_D - A_7)A_8 + \sigma_2\sigma_1)A_3 + A_8\alpha_1\lambda_D\phi_1\theta_1\varepsilon_1},$$

$$V_H^{**} = -\frac{\pi_H A_3 A_4 A_5 A_9 \sigma_1}{A_5 A_9 A_4((-\lambda_D - A_7)A_8 + \sigma_2\sigma_1)A_3 + A_8\alpha_1\lambda_D\phi_1\theta_1\varepsilon_1},$$

$$E_D^{**} = -\frac{\lambda_D \pi_H A_4 A_5 A_9 A_8}{A_5 A_9 A_4((-\lambda_D - A_7)A_8 + \sigma_2\sigma_1)A_3 + A_8\alpha_1\lambda_D\phi_1\theta_1\varepsilon_1},$$

$$I_D^{**} = -\frac{\lambda_D \pi_H A_5 A_9 A_8 \varepsilon_1}{A_5 A_9 A_4((-\lambda_D - A_7)A_8 + \sigma_2\sigma_1)A_3 + A_8\alpha_1\lambda_D\phi_1\theta_1\varepsilon_1},$$

$$T_D^{**} = -\frac{\lambda_D \pi_H A_9 A_8 \varepsilon_1 \phi_1}{A_5 A_9 A_4((-\lambda_D - A_7)A_8 + \sigma_2\sigma_1)A_3 + A_8\alpha_1\lambda_D\phi_1\theta_1\varepsilon_1},$$

$$R_D^{**} = \frac{\lambda_D \pi_H A_8 \varepsilon_1 \phi_1 \alpha_1}{A_3 A_4 A_5 A_7 A_8 A_9 + A_3 A_4 A_5 A_8 A_9 \lambda_D - A_3 A_4 A_5 A_9 \sigma_1 \sigma_2 - A_8 \alpha_1 \lambda_D \phi_1 \theta_1 \varepsilon_1},$$

$$S_{VD}^{**}=\pi_D\left(\begin{array}{l}\frac{\beta_{VD}\lambda_D A_5A_9A_8\varepsilon_1}{A_3A_4A_5A_8A_9+A_3A_4A_5A_9\sigma_1+A_4A_5A_8A_9\lambda_D+A_5A_8A_9\lambda_D\varepsilon_1+A_8A_9\lambda_D\phi_1\varepsilon_1}+\mu_{VD}\\ +A_8\alpha_1\lambda_D\phi_1\varepsilon_1\end{array}\right)^{-1},$$

$$I_{VD}^{**}=\frac{\pi_D\beta_{VD}\lambda_D A_5A_9A_8\varepsilon_1}{\left(\begin{array}{l}\left(\left(\left(\left(\left(\varepsilon_1+A_4\right)A_5+\varepsilon_1\phi_1\right)\mu_{VD}+\beta_{VD}\varepsilon_1A_5\right)\lambda_D+A_3A_4A_5\mu_{VD}\right)A_9+\lambda_D\varepsilon_1\mu_{VD}\phi_1\alpha_1\right)A_8\\ +A_3A_4A_5A_9\sigma_1\mu_{VD}\end{array}\right)A_6}$$

Substituting them into the force of infection for malaria $\lambda_D^{**}=\frac{b\beta_D I_{VD}}{N_H}$ and the force of infection for the vector$\lambda_{VD}^{**}=\frac{\beta_{VD}I_D}{N_H}$.

We obtained the following:

$f(\lambda)^{**}=\lambda^{**}\left(E^{2**}+F\lambda^{**}+G\right)=0$ and $\lambda^{**}=0$

denotes the disease free equilibrium point of the malaria Model.

Where

$$\begin{aligned}E=&-\pi_H{A_4}^2{A_5}^2A_6{A_8}^2{A_9}^2\mu_{VD}-\pi_HA_4{A_5}^2A_6{A_8}^2{A_9}^2\beta_{VD}\varepsilon_1-2\pi_HA_4{A_5}^2A_6{A_8}^2{A_9}^2\mu_{VD}\varepsilon_1\\&-2\pi_HA_4A_5A_6{A_8}^2{A_9}^2\mu_{VD}\phi_1\varepsilon_1-2\pi_HA_4A_5A_6{A_8}^2A_9\alpha_1\mu_{VD}\phi_1\varepsilon_1-\pi_H{A_5}^2A_6{A_8}^2{A_9}^2\beta_{VD}{\varepsilon_1}^2\\&-\pi_H{A_5}^2A_6{A_8}^2{A_9}^2\mu_{VD}{\varepsilon_1}^2-\pi_HA_5A_6{A_8}^2{A_9}^2\beta_{VD}\phi_1{\varepsilon_1}^2-2\pi_HA_5A_6{A_8}^2{A_9}^2\mu_{VD}\phi_1{\varepsilon_1}^2\\&-\pi_HA_5A_6{A_8}^2A_9\alpha_1\beta_{VD}\phi_1{\varepsilon_1}^2-2\pi_HA_5A_6{A_8}^2A_9\alpha_1\mu_{VD}\phi_1{\varepsilon_1}^2-\pi_HA_6{A_8}^2{A_9}^2\mu_{VD}{\phi_1}^2{\varepsilon_1}^2\\&-2\pi_HA_6{A_8}^2A_9\alpha_1\mu_{VD}{\phi_1}^2{\varepsilon_1}^2-\pi_HA_6{A_8}^2{\alpha_1}^2\mu_{VD}{\phi_1}^2{\varepsilon_1}^2\end{aligned}$$

$$\begin{aligned}F=&\pi_DA_3A_4{A_5}^2{A_8}^2{A_9}^2b\beta_D\beta_{VD}\varepsilon_1-\pi_DA_5{A_8}^2{A_9}^2b\alpha_1\beta_D\beta_{VD}\phi_1\theta_1{\varepsilon_1}^2-2\pi_HA_3{A_4}^2{A_5}^2A_6{A_8}^2{A_9}^2\mu_{VD}\\&-2\pi_HA_3{A_4}^2{A_5}^2A_6A_8{A_9}^2\mu_{VD}\sigma_1-\pi_HA_3A_4{A_5}^2A_6{A_8}^2{A_9}^2\beta_{VD}\varepsilon_1-2\pi_HA_3A_4{A_5}^2A_6{A_8}^2{A_9}^2\mu_{VD}\varepsilon_1\\&-\pi_HA_3A_4{A_5}^2A_6A_8{A_9}^2\beta_{VD}\sigma_1\varepsilon_1-2\pi_HA_3A_4A_5{}^2A_6A_8A_9{}^2\mu_{VD}\sigma_1\varepsilon_1-2\pi_HA_3A_4A_5A_6{A_8}^2{A_9}^2\mu_{VD}\phi_1\varepsilon_1\\&-2\pi_HA_3A_4A_5A_6{A_8}^2A_9\alpha_1\mu_{VD}\phi_1\varepsilon_1-2\pi_HA_3A_4A_5A_6A_8{A_9}^2\mu_{VD}\phi_1\sigma_1\varepsilon_1-2\pi_HA_3A_4A_5A_6A_8A_9\alpha_1\mu_{VD}\phi_1\sigma_1\varepsilon_1\end{aligned}$$

$$G=A_3A_4A_5^2A_9^2\left(1-(R_0^D)^2\right)$$

Thus for λ^{**} to be positive at the endemic equilibrium point, $R_0^D-1>0$.

$\Rightarrow R_0^D>1$and the endemic equilibrium point is stable.

Where

$A_3=\left(\varepsilon_1+\mu_H\right),A_4=\left(\phi_1+\delta_1+\mu_H\right),A_5=\left(\alpha_1+\delta_3+\mu_H\right),A_6=\left(\delta_{VD}+\mu_{VD}\right),A_7=\left(\sigma_1+\mu_H\right),A_8=\left(\sigma_2+\mu_H\right),A_9=\left(\theta_1+\mu_H\right).$ □

3.6. **Endemic Equilibrium of the malaria Sub-model.**

Theorem 4. *When $R_0^H < 1$, the endemic equilibrium point is unstable, while for $R_0^H > 1$, it is locally asymptotically stable.*

Proof. We solve for each of the model's state variables and set all of the model's equations to zero to obtain the following:

$$
\begin{aligned}
S_H^{**} &= -\frac{\pi_H B_3 B_4 B_5 B_8 B_9}{B_5 B_9((-\lambda_M - B_7)B_8 + \sigma_1\sigma_2)B_4 B_3 + B_8\alpha_3\lambda_M\phi_3\theta_2\varepsilon_2},\\
V_H^{**} &= -\frac{\pi_H B_3 B_4 B_5 B_9 \sigma_1}{B_5 B_9((-\lambda_M - B_7)B_8 + \sigma_1\sigma_2)B_4 B_3 + B_8\alpha_3\lambda_M\phi_3\theta_2\varepsilon_2},\\
E_M^{**} &= -\frac{\lambda_M\pi_H B_4 B_5 B_9 B_8}{B_5 B_9((-\lambda_M - B_7)B_8 + \sigma_1\sigma_2)B_4 B_3 + B_8\alpha_3\lambda_M\phi_3\theta_2\varepsilon_2},\\
I_M^{**} &= -\frac{\lambda_M\pi_H B_5 B_9 B_8\varepsilon_2}{B_5 B_9((-\lambda_M - B_7)B_8 + \sigma_1\sigma_2)B_4 B_3 + B_8\alpha_3\lambda_M\phi_3\theta_2\varepsilon_2},\\
T_M^{**} &= -\frac{\lambda_M\pi_H B_9 B_8\varepsilon_2\phi_3}{B_5 B_9((-\lambda_M - B_7)B_8 + \sigma_1\sigma_2)B_4 B_3 + B_8\alpha_3\lambda_M\phi_3\theta_2\varepsilon_2},\\
R_M^{**} &= \frac{\lambda_M\pi_H B_8\varepsilon_2\phi_3\alpha_3}{B_3 B_4 B_5 B_7 B_8 B_9 + B_3 B_4 B_5 B_8 B_9\lambda_M - B_3 B_4 B_5 B_9\sigma_1\sigma_2 - B_8\alpha_3\lambda_M\phi_3\theta_2\varepsilon_2},\\
S_{VM}^{**} &= \frac{\pi_M(B_3 B_4 B_5 B_8 B_9 + B_3 B_4 B_5 B_9\sigma_1 + B_4 B_5 B_8 B_9\lambda_M + B_5 B_8 B_9\lambda_M\varepsilon_2 + B_8 B_9\lambda_M\phi_3\varepsilon_2 + B_8\alpha_3\lambda_M\phi_3\varepsilon_2)}{B_3 B_4 B_5 B_8 B_9\mu_{VM} + B_3 B_4 B_5 B_9\mu_{VM}\sigma_1}\\
&\quad + B_4 B_5 B_8 B_9\lambda_M\mu_{VM} + \beta_{VM}\lambda_M B_5 B_9 B_8\varepsilon_2 + B_5 B_8 B_9\lambda_M\mu_{VM}\varepsilon_2\\
&\quad + B_8 B_9\lambda_M\mu_{VM}\phi_3\varepsilon_2 + B_8\alpha_3\lambda_M\mu_{VM}\phi_3\varepsilon_2
\end{aligned}
$$

$$
I_{VM}^{**} = \frac{\pi_M\beta_{VM}\lambda_M B_5 B_9 B_8\varepsilon_2}{\left(\begin{array}{l}(((((\varepsilon_2 + B_4)B_5 + \varepsilon_2\phi_3)\mu_{VM} + \beta_{VM}\varepsilon_2 B_5)\lambda_M + B_3 B_4 B_5\mu_{VM})B_9 + \lambda_M\varepsilon_2\mu_{VM}\phi_3\alpha_3)B_8\\ + B_3 B_4 B_5 B_9\mu_{VM}\sigma_1\end{array}\right)B_6},
$$

Substituting them into the force of infection for malaria $\lambda_M^{**} = \frac{b\beta_M I_{VM}}{N_H}$ and the force of infection for the vector$\lambda_{VM}^{**} = \frac{\beta_{VM} I_M}{N_H}$

We obtained the following:

$f(\lambda)^{**} = \lambda^{**}\left(H^{2**} + J\lambda^{**} + K\right) = 0$
and $\lambda^{**} = 0$

denotes the disease free equilibrium point of the malaria Model.

Where;

$$
\begin{aligned}
H &= \pi_H {B_4}^2 {B_5}^2 B_6 {B_8}^2 {B_9}^2\mu_{VM} + \pi_H B_4 {B_5}^2 B_6 {B_8}^2 {B_9}^2\beta_{VM}\varepsilon_2 + 2\pi_H B_4 {B_5}^2 B_6 {B_8}^2 {B_9}^2\mu_{VM}\varepsilon_2\\
&\quad + 2\pi_H B_4 B_5 B_6 {B_8}^2 {B_9}^2\mu_{VM}\phi_3\varepsilon_2 + 2\pi_H B_4 B_5 B_6 {B_8}^2 B_9\alpha_3\mu_{VM}\phi_3\varepsilon_2 + \pi_H {B_5}^2 B_6 {B_8}^2 {B_9}^2\beta_{VM}{\varepsilon_2}^2\\
&\quad + \pi_H {B_5}^2 B_6 {B_8}^2 {B_9}^2\mu_{VM}{\varepsilon_2}^2 + \pi_H B_5 B_6 {B_8}^2 {B_9}^2\beta_{VM}\phi_3{\varepsilon_2}^2 + 2\pi_H B_5 B_6 {B_8}^2 {B_9}^2\mu_{VM}\phi_3{\varepsilon_2}^2\\
&\quad + \pi_H B_5 B_6 {B_8}^2 B_9\alpha_3\beta_{VM}\phi_3{\varepsilon_2}^2 2\pi_H B_5 B_6 {B_8}^2 B_9\alpha_3\mu_{VM}\phi_3{\varepsilon_2}^2 + \pi_H B_6 {B_8}^2 {B_9}^2\mu_{VM}{\phi_3}^2{\varepsilon_2}^2\\
&\quad + 2\pi_H B_6 {B_8}^2 B_9\alpha_3\mu_{VM}{\phi_3}^2{\varepsilon_2}^2 + \pi_H B_6 {B_8}^2{\alpha_3}^2\mu_{VM}{\phi_3}^2{\varepsilon_2}^2
\end{aligned}
$$

$$J = -\pi_M B_3 B_4 {B_5}^2 {B_8}^2 {B_9}^2 b\beta_M \beta_{VM} \varepsilon_2 + \pi_M B_5 {B_8}^2 B_9 b\alpha_3 \beta_M \beta_{VM} \phi_3 \theta_2 {\varepsilon_2}^2 + 2\pi_H B_3 {B_4}^2 {B_5}^2 B_6 {B_8}^2 {B_9}^2 \mu_{VM}$$
$$+ 2\pi_H B_3 {B_4}^2 {B_5}^2 B_6 B_8 {B_9}^2 \mu_{VM} \sigma_1 + \pi_H B_3 B_4 {B_5}^2 B_6 {B_8}^2 {B_9}^2 \beta_{VM} \varepsilon_2 + 2\pi_H B_3 B_4 {B_5}^2 B_6 {B_8}^2 {B_9}^2 \mu_{VM} \varepsilon_2$$
$$+ \pi_H B_3 B_4 {B_5}^2 B_6 B_8 {B_9}^2 \beta_{VM} \sigma_1 \varepsilon_2 + 2\pi_H B_3 B_4 {B_5}^2 B_6 B_8 {B_9}^2 \mu_{VM} \sigma_1 \varepsilon_2 + 2\pi_H B_3 B_4 B_5 B_6 {B_8}^2 {B_9}^2 \mu_{VM} \phi_3 \varepsilon_2$$
$$2\pi_H B_3 B_4 B_5 B_6 {B_8}^2 B_9 \alpha_3 \mu_{VM} \phi_3 \varepsilon_2 + 2\pi_H B_3 B_4 B_5 B_6 B_8 {B_9}^2 \mu_{VM} \phi_3 \sigma_1 \varepsilon_2$$
$$+ 2\pi_H B_3 B_4 B_5 B_6 B_8 B_9 \alpha_3 \mu_{VM} \phi_3 \sigma_1 \varepsilon_2$$

$$K = \left(B_3 B_4 B_5^2 B_9^2\right) \pi_H B_3 B_4 B_6 \mu_{VM} (B_8 + \sigma_1)^2 \left(1 - (R_0^M)^2\right)$$

□

3.7. **Data fitting and parameter estimation of the malaria - dengue fever co-infection model.**

3.7.1. *Rationale for Data Selection.* Annual reported cases of malaria and dengue fever in Brazil from 2011 to 2023 (13 annual data points) were selected for parameter estimation. Brazil experiences the co-circulation of both vector-borne diseases, with malaria predominantly in the Amazon region (99% of national burden) and dengue affecting urban and peri-urban areas nationwide due to the expanding range of *Aedes aegypti*. The 13-year period captures contrasting long-term trends: a sustained decline in malaria cases (from 262,000 in 2011 to 125,000 in 2023, driven by enhanced surveillance, vector control, and interventions), alongside recurrent dengue epidemics with major peaks in 2013, 2015, and especially 2023 (>1.6 million cases). Data sources include Sivep-Malaria (autochthonous malaria cases, primarily *P. vivax* and *P. falciparum*) and SINAN (probable dengue notifications), providing nationally consistent surveillance records. While dedicated co-infection incidence data remain scarce, separate disease time series enable calibration of sub-models as a foundation for a full co-infection framework.

Table 3. Annual Malaria Cases in Brazil (2011–2023)

Year	Malaria Cases
2011	262,000
2012	241,000
2013	209,000
2014	177,000
2015	156,000
2016	130,000
2017	194,000
2018	193,000
2019	159,000
2020	146,000
2021	141,000
2022	131,000
2023	125,000

Data Source: Sivep-Malaria, Brazilian Ministry of Health. https://journals.plos.org/globalpublichealth/article?id=10.1371/journal.pgph.0002845

TABLE 4. Annual Dengue Cases in Brazil (2011–2023)

Year	Dengue Cases
2011	764,000
2012	590,000
2013	1,452,000
2014	592,000
2015	1,688,000
2016	1,500,000
2017	252,000
2018	265,000
2019	1,015,000
2020	983,000
2021	545,000
2022	1,454,000
2023	1,659,000

Data Source: Brazilian Ministry of Health / SINAN (Notifiable Diseases Information System). https://pmc.ncbi.nlm.nih.gov/articles/PMC11415067/

3.7.2. *Data Fitting Methodology.* The fitting calibrated separate malaria and dengue submodels against monthly-interpolated case series (156 months, January 2011–December 2023) derived from the annual data above, with seasonal adjustments applied (rainy-season weighting for malaria, January–May peak weighting for dengue). Eleven key parameters per submodel were estimated simultaneously using the Trust Region Reflective (`trf`) algorithm in `scipy.optimize.least_squares`, minimizing squared residuals between simulated and observed monthly new cases.

Fitted parameters are listed in Table 5. The ODE systems were solved with `scipy.integrate.odeint` over a dense temporal grid (1560 points across 13 years). New cases were derived from the force-of-infection flow into exposed compartments and aggregated monthly via trapezoidal integration. Fixed values included Brazil's human population (214 million), vector population estimates (Anopheles 1×10^9, Aedes 2×10^9), natural death rates, recruitment rates, and biting rates (0.5 for malaria, 0.7 for dengue vectors).

Model performance was evaluated using multiple metrics on the monthly scale (n=156):

For **Malaria**:

R^2 = -17.2661

For **Dengue**:

R^2 = -3.8399

Negative R^2 values indicate that the current sub-models explain less variance than a simple mean prediction, likely due to dengue's explosive epidemic behavior (not fully captured without serotype or climate drivers), imperfect seasonal disaggregation, potential underreporting, and the lack of explicit co-infection dynamics or cross-effects in these separate fits.

The visual comparison of observed versus fitted monthly cases is shown in Figures 2 and 3.

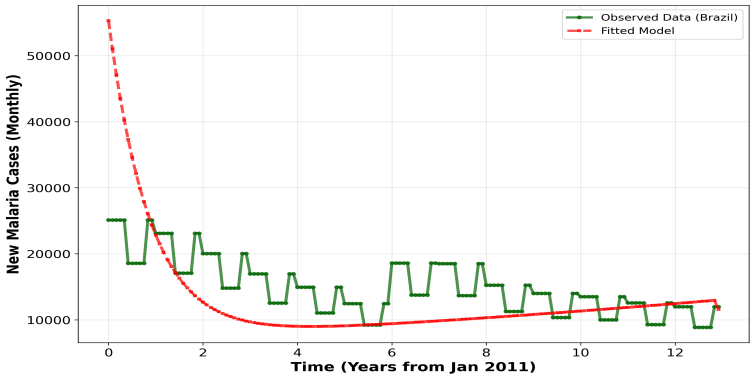

FIGURE 2. **Model fit to monthly malaria cases in Brazil (2011–2023).** Observed data (green line with circles) show the long-term decline with seasonal fluctuations. Fitted model output (red dashed line with squares) is shown for comparison. While the general decreasing trend is partially captured, discrepancies are evident, contributing to the negative R^2.

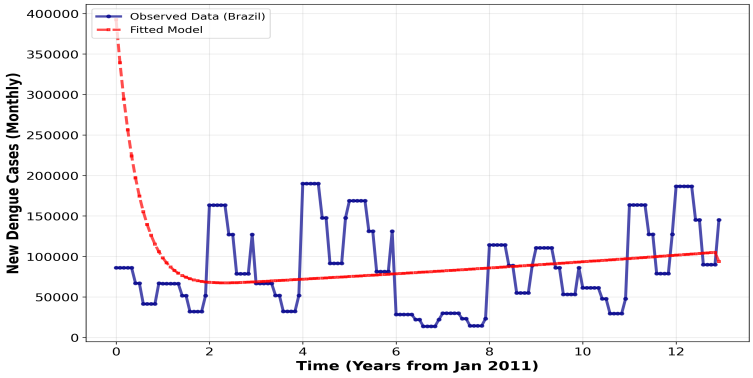

FIGURE 3. **Model fit to monthly dengue cases in Brazil (2011–2023).** Observed data (blue line with circles) exhibit recurrent large epidemics (e.g., 2015, 2022–2023 peaks). Fitted model output (red dashed line with squares) struggles to reproduce sharp outbreak dynamics, reflected in the negative R^2 value.

TABLE 5. Fitted parameter values for the malaria and dengue sub-models (Brazil, 2011–2023)

Parameter	Value
β_d	0.080000
β_m	0.120000
β_{vd}	0.200000
β_{vm}	0.250000
ε_1	0.200000
ε_2	0.170000
ϕ_1	0.150000
ϕ_2	0.120000
ϕ_3	0.130000
α_1	0.080000
α_2	0.060000
α_3	0.070000
θ_1	0.006000
θ_2	0.003000
δ_1	0.001000
δ_2	0.002000
δ_3	0.015000
δ_4	0.020000
δ_5	0.025000
δ_6	0.015000
σ_1	0.030000
σ_2	0.020000

These results serve as a baseline for extending the framework to include explicit malaria-dengue co-infection compartments, cross-immunity, enhanced seasonality (e.g., climate covariates), or joint optimization of shared parameters to improve overall fit quality.

3.8. **Sensitivity Analysis of the Dengue only Model.** Sensitivity analysis is used to identify the factors that promote both the control and spread of an infection within a population. The following represents the sensitivity index of the Dengue model's reproduction number with respect to any given parameter, let's say p:

$$\Upsilon_p^{R_0} = \frac{\partial R_0}{\partial p} \times \frac{p}{R_0}$$

Given that

$$R_0 = \frac{\sqrt{\mu_{VD}\pi_H A_3 A_4 A_2 A_6 \beta_{VD}\pi_D \mu_H \varepsilon_3 b \beta_D A_1}}{\mu_{VD}\pi_H A_3 A_4 A_2 A_6}$$

$\Im_{\pi_H}^{R_0} = -0.5,$
$\Im_{\varepsilon_1}^{R_0} = -\frac{\varepsilon_1}{2\varepsilon_1+2\mu_H} = -0.4999,$
$\Im_{\phi_1}^{R_0} = -\frac{\phi_1}{2\phi_1+2\delta_1+2\mu_H} = -0.4808,$
$\Im_{\delta_1}^{R_0} = -\frac{\delta_1}{2\phi_1+2\delta_1+2\mu_H} = -0.0190,$
$\Im_{\sigma_1}^{R_0} = -\frac{\sigma_1}{2\sigma_1+2\sigma_2+2\mu_H} = -0.4261,$
$\Im_{\sigma_2}^{R_0} = 1/2\frac{\sigma_1\sigma_2}{(\sigma_1+\sigma_2+\mu_H)(\mu_H+\sigma_2)} = 0.4259,$
$\Im_{\delta_{VD}}^{R_0} = -\frac{\delta_{VD}}{2\delta_{VD}+2\mu_{VD}} = -0.3497,$
$\Im_{\beta_{VD}}^{R_0} = 0.5,$
$\Im_{\varepsilon_3}^{R_0} = 0.5,$
$\Im_{\pi_D}^{R_0} = 0.5,$
$\Im_{\pi_D}^{R_0} = \frac{-\delta_{VD}-2\mu_{VD}}{2\delta_{VD}+2\mu_{VD}} = -0.6503,$
$\Im_{\mu_H}^{R_0} = \frac{-\delta_{VD}-2\mu_{VD}}{2\delta_{VD}+2\mu_{VD}} = -0.4999.$

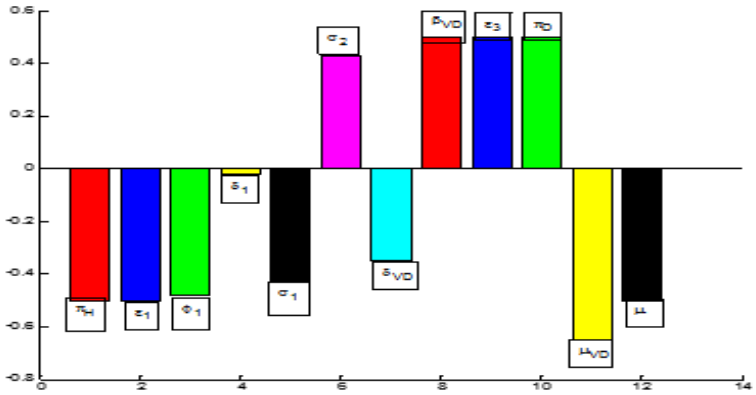

FIGURE 4. Sensitivity barchart of the dengue fever sub-model

Based on the sensitivity analysis of the Dengue only model, the parameters with positive sensitivity indices which are $\sigma_2, \beta_{VD}, \varepsilon_3, \pi_D$
increases the incidence of Dengue in the human population Conversely, the parameters $\varepsilon_1, \pi_H, \phi_1, \delta_1, \sigma_1, \delta_{VD}, \mu_{VD}$.
Negative sensitivity indices are known to diminish the prevalence of tuberculosis among the human population.

3.8.1. *Sensitivity Analysis of the Malaria only Model.* Sensitivity analysis is used to identify the factors that promote both the control and spread of an infection within a population. The following represents the sensitivity index of the malaria model's reproduction number with

respect to any given parameter, let's say p:

$$\Im_q^{R_0} = \frac{\partial R_0}{\partial q} \times \frac{q}{R_0}$$

Given that

$$R_0 = \frac{\sqrt{\mu_{VM}\pi_H B_3 B_4 B_2 B_6 \beta_{VM} \Lambda_m \mu_H \varepsilon_2 b \beta_m B_1}}{\mu_{VM}\pi_H B_3 B_4 B_2 B_6}$$

$$\aleph_{\pi_H}^{R_0} = -0.5,$$
$$\aleph_{\varepsilon_2}^{R_0} = \frac{\mu_H}{2\varepsilon_2+2\mu_H} = 0.0002,$$
$$\aleph_{\phi_3}^{R_0} = -\frac{\phi_3}{2\phi_3+2\delta_2+2\mu_H} = -0.4164,$$
$$\aleph_{\delta_2}^{R_0} = -\frac{\delta_2}{2\phi_3+2\delta_2+2\mu_H} = -0.0828,$$
$$\aleph_{\sigma_1}^{R_0} = -\frac{\sigma_1}{2\sigma_1+2\sigma_2+2\mu_H} = -0.3770,$$
$$\aleph_{\beta_{VM}}^{R_0} = -\frac{\delta_{VM}}{2\delta_{VM}+2\mu_{VM}} = -0.0904,$$
$$\aleph_b^{R_0} = 0.5,$$
$$\aleph_{\mu_H}^{R_0} = -0.9945,$$
$$\aleph_{\sigma_2}^{R_0} = 1/2\frac{\sigma_1\sigma_2}{(\sigma_1+\sigma_2+\mu_H)(\mu_H+\sigma_2)} = 0.3769$$

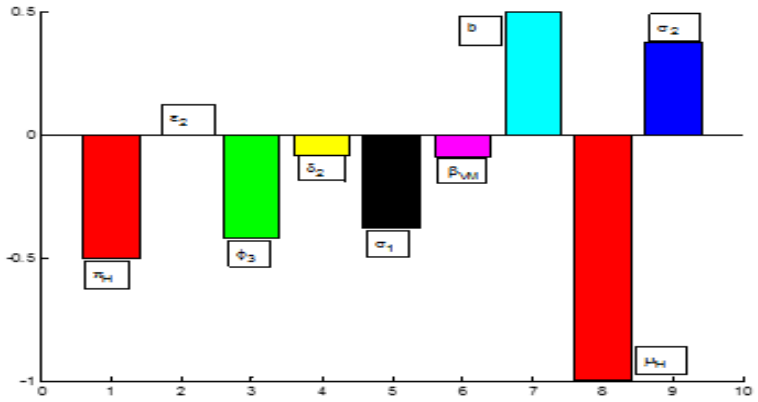

FIGURE 5. Sensitivity barchart of the malaria sub-model

Based on the sensitivity analysis of the Malaria only model, the parameters with positive sensitivity indices which are $b, \sigma_2, \varepsilon_2$
increases the incidence of Dengue in the human population Conversely, the parameters $\pi_H, \phi_3, \delta_2, \sigma_1, \beta_{VD}, \mu_H,$

Negative sensitivity indices are known to diminish the prevalence of tuberculosis among the human population.

4. Optimal Control Strategy for Reducing Disease Burden

The concept of "optimal control strategy" refers to implementing optimal interventions for managing infectious disease transmission dynamics through various scientific approaches. This methodology has proven essential in identifying effective strategies for controlling harmful communicable diseases. The primary objective is to determine an approach that minimizes both the number of infected individuals and the associated intervention costs.

For the malaria-dengue fever co-infection model, we introduce six time-varying control measures:

$(u_1(t), u_2(t), u_3(t), u_4(t), u_5(t), u_6(t))$, representing:

- $u_1(t)$: Insecticide-treated bed net (ITN) usage rate for malaria prevention
- $u_2(t)$: Indoor residual spraying (IRS) effectiveness for malaria vector control
- $u_3(t)$: Environmental management and larvicide application rate for dengue vector control
- $u_4(t)$: Personal protection measures (mosquito repellents, protective clothing) compliance rate
- $u_5(t)$: Treatment compliance rate for co-infected individuals
- $u_6(t)$: Vaccination rate of susceptible individuals against malaria

Detailed Parameter Descriptions. $u_1(t)$: This parameter represents the compliance rate for insecticide-treated bed net usage, a critical intervention for reducing malaria transmission through mosquito bites during sleeping hours. Quantification considers factors such as net distribution coverage, community acceptance, proper usage patterns, and net durability.

$u_2(t)$: Indoor residual spraying serves as a key malaria vector control measure by reducing mosquito populations within households. This parameter accounts for spray coverage, chemical efficacy, reapplication schedules, and community acceptance of spraying programs.

$u_3(t)$: Environmental management targeting dengue vector breeding sites is fundamental for dengue control. Quantification involves assessing larvicide application frequency, community participation in removing standing water, and effectiveness of source reduction activities.

$u_4(t)$: Personal protection measures including mosquito repellent usage and protective clothing are vital for both diseases. This parameter considers product availability, public awareness levels, socioeconomic factors affecting usage, and compliance patterns throughout the day.

$u_5(t)$: Treatment compliance for co-infected individuals is crucial given the complexity of managing dual infections. Quantification addresses healthcare accessibility, medication adherence, treatment protocol complexity, and patient monitoring systems.

$u_6(t)$: Vaccination of susceptible individuals against malaria represents a preventive intervention. This parameter encompasses vaccine supply logistics, distribution infrastructure, vaccine acceptance rates, dosing schedules, and priority group identification.

Controlled Model System. Incorporating these control measures, the malaria-dengue fever co-infection model transforms into:

$$\frac{dS_H}{dt} = \pi_H + \theta_1 R_D + \theta_2 R_M + \sigma_2 V_H - (1-u_1(t))(1-u_2(t))\lambda_D S_H$$

$$-(1-u_1(t))(1-u_2(t))\lambda_M S_H - (\sigma_1 + \mu_H)S_H - u_6(t)S_H,$$

$$\frac{dE_D}{dt} = (1-u_1(t))(1-u_2(t))\lambda_D S_H - (1-u_4(t))\lambda_M E_D - (\varepsilon_1 + \mu_H)E_D,$$

$$\frac{dE_M}{dt} = (1-u_1(t))(1-u_2(t))\lambda_M S_H - (1-u_4(t))\lambda_D E_M - (\varepsilon_2 + \mu_H)E_M,$$

$$\frac{dE_{DM}}{dt} = (1-u_4(t))\lambda_M E_D + (1-u_4(t))\lambda_D E_M - (\varepsilon_3 + \mu_H)E_{DM},$$

$$\frac{dI_D}{dt} = \varepsilon_1 E_D - (\phi_1 + \varepsilon_4 + \delta_1 + \mu_H)I_D,$$

$$\frac{dI_M}{dt} = \varepsilon_2 E_M - (\phi_3 + \varepsilon_5 + \delta_2 + \mu_H)I_M,$$

$$\frac{dI_{DM}}{dt} = \varepsilon_3 E_{DM} + \varepsilon_4 I_D + \varepsilon_5 I_M - ((1-u_5(t))\phi_2 + \delta_5 + \mu_H)I_{DM},$$

$$\frac{dT_D}{dt} = \phi_1 I_D - (\alpha_1 + \delta_3 + \mu_H)T_D,$$

$$\frac{dT_M}{dt} = \phi_3 I_M - (\alpha_3 + \delta_4 + \mu_H)T_M,$$

$$\frac{dT_{DM}}{dt} = (1-u_5(t))\phi_2 I_{DM} - \alpha_2 T_{DM} - (\delta_6 + \mu_H)T_{DM},$$

$$\frac{dV_H}{dt} = \sigma_1 S_H + u_6(t)S_H - (\sigma_2 + \mu_H)V_H,$$

$$\frac{dR_D}{dt} = \alpha_1 T_D - (\theta_1 + \mu_H)R_D,$$

$$\frac{dR_M}{dt} = \alpha_3 T_M - (\theta_2 + \mu_H)R_M,$$

$\frac{dR_{DM}}{dt} = \alpha_2 T_{DM} - \mu_H R_{DM},$

$\frac{dS_{VM}}{dt} = \pi_M - (1 - u_2(t))\lambda_{VM} S_{VM} - \mu_{VM} S_{VM},$

$\frac{dI_{VM}}{dt} = (1 - u_2(t))\lambda_{VM} S_{VM} - (\delta_{VM} + \mu_{VM}) I_{VM},$

$\frac{dS_{VD}}{dt} = \pi_D - (1 - u_3(t))\lambda_{VD} S_{VD} - \mu_{VD} S_{VD},$

$\frac{dI_{VD}}{dt} = (1 - u_3(t))\lambda_{VD} S_{VD} - (\delta_{VD} + \mu_{VD}) I_{VD}.$

Where the force of infection terms remain:

$$\lambda_D = \frac{b\beta_D I_{VD}}{N_H}, \quad \lambda_M = \frac{b\beta_M I_{VM}}{N_H}, \quad \lambda_{VM} = \frac{\beta_{VM}(I_M + I_{DM})}{N_H}, \quad \lambda_{VD} = \frac{\beta_{VD}(I_D + I_{DM})}{N_H}.$$

Objective Functional. Following established optimal control theory frameworks, we define the objective functional to minimize disease burden and intervention costs:

$$J[u_1, u_2, u_3, u_4, u_5, u_6] = \int_0^{t_f} \left[A_1 I_D + A_2 I_M + A_3 I_{DM} + \frac{1}{2} \sum_{i=1}^{6} A_{i+3} u_i^2(t) \right] dt$$

where A_i, $(i = 1, 2, \ldots, 9)$ are positive weighting constants balancing the objective functional components. For our analysis, we assign unit values to these weights. The integrand components represent:

(1) $A_1 I_D + A_2 I_M + A_3 I_{DM}$: Costs associated with managing infected individuals in each disease category
(2) $A_4 u_1^2(t)$: Cost of implementing and maintaining ITN distribution and usage programs
(3) $A_5 u_2^2(t)$: Cost of indoor residual spraying programs including chemicals and labor
(4) $A_6 u_3^2(t)$: Cost of environmental management and larvicide applications for dengue control
(5) $A_7 u_4^2(t)$: Cost of personal protection measure distribution and awareness campaigns
(6) $A_8 u_5^2(t)$: Cost of enhanced treatment protocols for co-infected patients
(7) $A_9 u_6^2(t)$: Cost of malaria vaccination program implementation

The goal is to minimize the total infected population across all disease categories while minimizing intervention costs. We seek optimal controls $(u_1^*(t), u_2^*(t), u_3^*(t), u_4^*(t), u_5^*(t), u_6^*(t))$ such that:

$$J[u_1^*, u_2^*, u_3^*, u_4^*, u_5^*, u_6^*] = \min_{u \in \Upsilon} J[u_1, u_2, u_3, u_4, u_5, u_6]$$

where the admissible control set is defined as:

$$\Upsilon = \left\{ (u_1, u_2, u_3, u_4, u_5, u_6) \in L^1(0, t_f)^6 \mid 0 \leqslant u_i(t) \leqslant 1,\ i = 1, 2, \ldots, 6,\ t \in [0, t_f] \right\}$$

4.1. **Theoretical Analysis of Optimal Control.** To determine the necessary conditions that an optimal control must fulfill, we employ Pontryagin's maximum principle. This fundamental theorem in optimal control theory serves as our analytical framework for examining the optimal control problem. The principle establishes necessary conditions for optimality, providing guidance in determining the optimal control strategy for the malaria-dengue fever co-infection model.

According to Pontryagin's Maximum Principle, the optimal control strategy must satisfy specific conditions. These conditions require that the Hamiltonian be minimized with respect to the control variables, while the co-state variables must satisfy a system of differential equations termed the adjoint equations. The Hamiltonian function represents the sum of the objective functional and the epidemiological model dynamics, weighted by Lagrange multipliers (referred to as co-state variables).

Through this methodology, the controlled system and objective functional are transformed into an optimization problem of minimizing the point-wise Hamiltonian ($\mathcal{H}$) with respect to the control vector $(u_1^*(t), u_2^*(t), u_3^*(t), u_4^*(t), u_5^*(t), u_6^*(t))$. The Hamiltonian is formulated as follows:

$$
\begin{aligned}
\mathcal{H} \;=\; & A_1 I_D + A_2 I_M + A_3 I_{DM} \\
& + \frac{1}{2}\left[A_4 u_1^2(t) + A_5 u_2^2(t) + A_6 u_3^2(t) + A_7 u_4^2(t) + A_8 u_5^2(t) + A_9 u_6^2(t)\right] \\
& + \lambda_1 \left[\pi_H + \theta_1 R_D + \theta_2 R_M + \sigma_2 V_H - (1-u_1(t))(1-u_2(t))\lambda_D S_H \right. \\
& \qquad \left. - (1-u_1(t))(1-u_2(t))\lambda_M S_H - (\sigma_1 + \mu_H) S_H - u_6(t) S_H\right] \\
& + \lambda_2 \left[(1-u_1(t))(1-u_2(t))\lambda_D S_H - (1-u_4(t))\lambda_M E_D - (\varepsilon_1 + \mu_H) E_D\right] \\
& + \lambda_3 \left[(1-u_1(t))(1-u_2(t))\lambda_M S_H - (1-u_4(t))\lambda_D E_M - (\varepsilon_2 + \mu_H) E_M\right] \\
& + \lambda_4 \left[(1-u_4(t))\lambda_M E_D + (1-u_4(t))\lambda_D E_M - (\varepsilon_3 + \mu_H) E_{DM}\right] \\
& + \lambda_5 \left[\varepsilon_1 E_D - (\phi_1 + \varepsilon_4 + \delta_1 + \mu_H) I_D\right] \\
& + \lambda_6 \left[\varepsilon_2 E_M - (\phi_3 + \varepsilon_5 + \delta_2 + \mu_H) I_M\right] \\
& + \lambda_7 \left[\varepsilon_3 E_{DM} + \varepsilon_4 I_D + \varepsilon_5 I_M - ((1-u_5(t))\phi_2 + \delta_5 + \mu_H) I_{DM}\right] \\
& + \lambda_8 \left[\phi_1 I_D - (\alpha_1 + \delta_3 + \mu_H) T_D\right] \\
& + \lambda_9 \left[\phi_3 I_M - (\alpha_3 + \delta_4 + \mu_H) T_M\right] \\
& + \lambda_{10} \left[(1-u_5(t))\phi_2 I_{DM} - \alpha_2 T_{DM} - (\delta_6 + \mu_H) T_{DM}\right] \\
& + \lambda_{11} \left[\sigma_1 S_H + u_6(t) S_H - (\sigma_2 + \mu_H) V_H\right] \\
& + \lambda_{12} \left[\alpha_1 T_D - (\theta_1 + \mu_H) R_D\right] \\
& + \lambda_{13} \left[\alpha_3 T_M - (\theta_2 + \mu_H) R_M\right] \\
& + \lambda_{14} \left[\alpha_2 T_{DM} - \mu_H R_{DM}\right] \\
& + \lambda_{15} \left[\pi_M - (1-u_2(t))\lambda_{VM} S_{VM} - \mu_{VM} S_{VM}\right]
\end{aligned}
$$

$$+\lambda_{16}\left[(1-u_2(t))\,\lambda_{VM}S_{VM}-(\delta_{VM}+\mu_{VM})\,I_{VM}\right]$$
$$+\lambda_{17}\left[\pi_D-(1-u_3(t))\,\lambda_{VD}S_{VD}-\mu_{VD}S_{VD}\right]$$
$$+\lambda_{18}\left[(1-u_3(t))\,\lambda_{VD}S_{VD}-(\delta_{VD}+\mu_{VD})\,I_{VD}\right] \tag{2}$$

Applying Pontryagin's maximum principle and the existence result for optimal control vectors $(u_1^*(t), u_2^*(t),\ u_3^*(t), u_4^*(t), u_5^*(t), u_6^*(t))$, we derive the corresponding theorem, where $\lambda_i, (i = 1, 2, 3, \ldots, 18)$ denote the adjoint functions corresponding to the state variables of the controlled malaria-dengue fever co-infection model.

Theorem 5. *There exist optimal control parameters $u_1^*(t)$, $u_2^*(t)$, $u_3^*(t)$, $u_4^*(t)$, $u_5^*(t)$ and $u_6^*(t)$ with corresponding optimal solution*
$(S_H^*, E_D^*, E_M^*, E_{DM}^*, I_D^*, I_M^*, I_{DM}^*, T_D^*, T_M^*, T_{DM}^*, V_H^*, R_D^*, R_M^*, R_{DM}^*, S_{VM}^*, I_{VM}^*, S_{VD}^*, I_{VD}^*)$ *that minimize*
$J\left(u_1^*(t), u_2^*(t), u_3^*(t), u_4^*(t), u_5^*(t), u_6^*(t)\right)$ *over* Υ. *Furthermore, there exist adjoint functions,* $\lambda_i, (i = 1, 2, 3, ..., 18)$ *satisfying:*

$$\begin{aligned}
\frac{d\lambda_1}{dt} =& -\frac{I_{VD}b\beta_D\lambda_2(u_1-1)(u_2-1)}{N_H}-\frac{I_{VM}b\beta_M\lambda_3(u_1-1)(u_2-1)}{N_H}\\
&+\left(\frac{I_{VD}b\beta_D(u_1-1)(u_2-1)}{N_H}+\frac{I_{VM}b\beta_M(u_1-1)(u_2-1)}{N_H}+\mu_H+\sigma_1+u_6\right)\lambda_1\\
&-\lambda_{11}(\sigma_1+u_6)\\
\frac{d\lambda_2}{dt} =& \frac{I_{VM}b\beta_M\lambda_4(u_4-1)}{N_H}-\left(\frac{I_{VM}b\beta_M(u_4-1)}{N_H}-\mu_H-\varepsilon_1\right)\lambda_2-\lambda_5\varepsilon_1\\
\frac{d\lambda_3}{dt} =& \frac{I_{VD}b\beta_D\lambda_4(u_4-1)}{N_H}-\left(\frac{I_{VD}b\beta_D(u_4-1)}{N_H}-\mu_H-\varepsilon_2\right)\lambda_3-\lambda_6\varepsilon_2\\
\frac{d\lambda_4}{dt} =& \lambda_4(\mu_H+\varepsilon_3)-\lambda_7\varepsilon_3\\
\frac{d\lambda_5}{dt} =& -\frac{S_{VD}\beta_{VD}\lambda_{17}(u_3-1)}{N_H}+\frac{S_{VD}\beta_{VD}\lambda_{18}(u_3-1)}{N_H}\\
&+(\delta_1+\mu_H+\phi_1+\varepsilon_4)\lambda_5-\lambda_8\phi_1-\lambda_7\varepsilon_4-A_1
\end{aligned}$$

$$\begin{aligned}
\frac{d\lambda_6}{dt} =& -\frac{S_{VM}\beta_{VM}\lambda_{15}(u_2-1)}{N_H}+\frac{S_{VM}\beta_{VM}\lambda_{16}(u_2-1)}{N_H}\\
&+(\delta_2+\mu_H+\phi_3+\varepsilon_5)\lambda_6-\lambda_9\phi_3-\lambda_7\varepsilon_5-A_2
\end{aligned} \tag{3}$$

$$\begin{aligned}
\frac{d\lambda_7}{dt} =& -\frac{S_{VM}\beta_{VM}\lambda_{15}(u_2-1)}{N_H}+\frac{S_{VM}\beta_{VM}\lambda_{16}(u_2-1)}{N_H}-\frac{S_{VD}\beta_{VD}\lambda_{17}(u_3-1)}{N_H}\\
&+\frac{S_{VD}\beta_{VD}\lambda_{18}(u_3-1)}{N_H}+\lambda_{10}\phi_2(u_5-1)-(\phi_2(u_5-1)-\delta_5-\mu_H)\lambda_7-A_3\\
\frac{d\lambda_8}{dt} =& -\alpha_1\lambda_{12}+(\alpha_1+\delta_3+\mu_H)\lambda_8
\end{aligned}$$

$$\frac{d\lambda_9}{dt} = -\alpha_3\lambda_{13} + (\alpha_3 + \delta_4 + \mu_H)\lambda_9$$

$$\frac{d\lambda_{10}}{dt} = (\alpha_2 + \delta_6 + \mu_H)\lambda_{10} - \alpha_2\lambda_{14}$$

$$\frac{d\lambda_{11}}{dt} = \lambda_{11}(\mu_H + \sigma_2) - \lambda_1\sigma_2$$

$$\frac{d\lambda_{12}}{dt} = \lambda_{12}(\mu_H + \theta_1) - \lambda_1\theta_1$$

$$\frac{d\lambda_{13}}{dt} = \lambda_{13}(\mu_H + \theta_2) - \lambda_1\theta_2$$

$$\frac{d\lambda_{14}}{dt} = \lambda_{14}\mu_H$$

$$\frac{d\lambda_{15}}{dt} = \frac{(I_{DM} + I_M)\beta_{VM}\lambda_{16}(u_2 - 1)}{N_H} - \left(\frac{(I_{DM} + I_M)\beta_{VM}(u_2 - 1)}{N_H} - \mu_{VM}\right)\lambda_{15}$$

$$\frac{d\lambda_{16}}{dt} = \frac{S_H b\beta_M\lambda_1(u_1 - 1)(u_2 - 1)}{N_H} - \frac{S_H b\beta_M\lambda_3(u_1 - 1)(u_2 - 1)}{N_H} - \frac{E_D b\beta_M\lambda_2(u_4 - 1)}{N_H} + \frac{E_D b\beta_M\lambda_4(u_4 - 1)}{N_H} + (\delta_{VM} + \mu_{VM})\lambda_{16}$$

$$\frac{d\lambda_{17}}{dt} = \frac{(I_D + I_{DM})\beta_{VD}\lambda_{18}(u_3 - 1)}{N_H} - \left(\frac{(I_D + I_{DM})\beta_{VD}(u_3 - 1)}{N_H} - \mu_{VD}\right)\lambda_{17}$$

$$\frac{d\lambda_{18}}{dt} = \frac{S_H b\beta_D\lambda_1(u_1 - 1)(u_2 - 1)}{N_H} - \frac{S_H b\beta_D\lambda_2(u_1 - 1)(u_2 - 1)}{N_H} - \frac{E_M b\beta_D\lambda_3(u_4 - 1)}{N_H} + \frac{E_M b\beta_D\lambda_4(u_4 - 1)}{N_H} + (\delta_{VD} + \mu_{VD})\lambda_{18}$$

With transversality conditions:

$$\lambda_i(t_f) = 0, \quad i = 1, 2, 3, ..., 18 \tag{4}$$

and

$$N_H^* = S_H^* + E_D^* + E_M^* + E_{DM}^* + I_D^* + I_M^* + I_{DM}^* + T_D^* + T_M^* + T_{DM}^* + V_H^* + R_D^* + R_M^* + R_{DM}^*$$

the following optimal control characterizations hold:

$$u_1^*(t) = \min\left(\max\left(0, \frac{I_{VD}S_H b\beta_D\lambda_2 + I_{VM}S_H b\beta_M\lambda_3 - (I_{VD}S_H b\beta_D + I_{VM}S_H b\beta_M)\lambda_1}{A_4 N_H} - \frac{(I_{VD}S_H b\beta_D\lambda_2 + I_{VM}S_H b\beta_M\lambda_3 - (I_{VD}S_H b\beta_D + I_{VM}S_H b\beta_M)\lambda_1)u_2}{A_4 N_H}\right), 1\right)$$

$$u_2^*(t) = \min\left(\max\left(0, \frac{I_{VD}S_H b\beta_D\lambda_2 + I_{VM}S_H b\beta_M\lambda_3 - (I_{DM} + I_M)S_{VM}\beta_{VM}\lambda_{15}}{A_5 N_H} + \frac{(I_{DM} + I_M)S_{VM}\beta_{VM}\lambda_{16} - (I_{VD}S_H b\beta_D + I_{VM}S_H b\beta_M)\lambda_1}{A_5 N_H} - \frac{(I_{VD}S_H b\beta_D\lambda_2 + I_{VM}S_H b\beta_M\lambda_3 - (I_{VD}S_H b\beta_D + I_{VM}S_H b\beta_M)\lambda_1)u_1}{A_5 N_H}\right), 1\right)$$

$$
\begin{aligned}
u_3^*(t) &= \min\left(\max\left(0, -\frac{(I_D+I_{DM})S_{VD}\beta_{VD}\lambda_{17}-(I_D+I_{DM})S_{VD}\beta_{VD}\lambda_{18}}{A_6N_H}\right),1\right)\\
u_4^*(t) &= \min\left(\max\left(0, -\frac{E_DI_{VM}b\beta_M\lambda_2+E_MI_{VD}b\beta_D\lambda_3-(E_MI_{VD}b\beta_D+E_DI_{VM}b\beta_M)\lambda_4}{A_7N_H}\right),1\right)\\
u_5^*(t) &= \min\left(\max\left(0, \frac{(I_{DM}\lambda_{10}-I_{DM}\lambda_7)\phi_2}{A_8}\right),1\right)\\
u_6^*(t) &= \min\left(\max\left(0, \frac{S_H\lambda_1-S_H\lambda_{11}}{A_9}\right),1\right) \qquad (5)
\end{aligned}
$$

Proposition 1. *The existence of an optimal control vector* $(u_1(t), u_2(t), u_3(t), u_4(t), u_5(t), u_6(t))$ *follows from Corollary 4.1 of Fleming and Rishel, owing to the convexity of the integrand of* J *with respect to* $(u_1, u_2, u_3, u_4, u_5, u_6)$*, the a priori boundedness of state solutions, and the Lipschitz continuity of the state system with respect to state variables.*

Proof. We apply Pontryagin's maximum principle to obtain:

$$\frac{d\lambda_1}{dt} = -\frac{\partial\mathcal{H}}{\partial S_H},\ \lambda_1(t_f)=0, \quad \frac{d\lambda_2}{dt} = -\frac{\partial\mathcal{H}}{\partial E_D},\ \lambda_2(t_f)=0, \quad \frac{d\lambda_3}{dt} = -\frac{\partial\mathcal{H}}{\partial E_M},\ \lambda_3(t_f)=0$$

$$\frac{d\lambda_4}{dt} = -\frac{\partial\mathcal{H}}{\partial E_{DM}},\ \lambda_4(t_f)=0, \quad \frac{d\lambda_5}{dt} = -\frac{\partial\mathcal{H}}{\partial I_D},\ \lambda_5(t_f)=0, \quad \frac{d\lambda_6}{dt} = -\frac{\partial\mathcal{H}}{\partial I_M},\ \lambda_6(t_f)=0$$

$$\frac{d\lambda_7}{dt} = -\frac{\partial\mathcal{H}}{\partial I_{DM}},\ \lambda_7(t_f)=0, \quad \frac{d\lambda_8}{dt} = -\frac{\partial\mathcal{H}}{\partial T_D},\ \lambda_8(t_f)=0, \quad \frac{d\lambda_9}{dt} = -\frac{\partial\mathcal{H}}{\partial T_M},\ \lambda_9(t_f)=0$$

$$\frac{d\lambda_{10}}{dt} = -\frac{\partial\mathcal{H}}{\partial T_{DM}},\ \lambda_{10}(t_f)=0, \quad \frac{d\lambda_{11}}{dt} = -\frac{\partial\mathcal{H}}{\partial V_H},\ \lambda_{11}(t_f)=0, \quad \frac{d\lambda_{12}}{dt} = -\frac{\partial\mathcal{H}}{\partial R_D},\ \lambda_{12}(t_f)=0$$

$$\frac{d\lambda_{13}}{dt} = -\frac{\partial\mathcal{H}}{\partial R_M},\ \lambda_{13}(t_f)=0, \quad \frac{d\lambda_{14}}{dt} = -\frac{\partial\mathcal{H}}{\partial R_{DM}},\ \lambda_{14}(t_f)=0, \quad \frac{d\lambda_{15}}{dt} = -\frac{\partial\mathcal{H}}{\partial S_{VM}},\ \lambda_{15}(t_f)=0$$

$$\frac{d\lambda_{16}}{dt} = -\frac{\partial\mathcal{H}}{\partial I_{VM}},\ \lambda_{16}(t_f)=0, \quad \frac{d\lambda_{17}}{dt} = -\frac{\partial\mathcal{H}}{\partial S_{VD}},\ \lambda_{17}(t_f)=0, \quad \frac{d\lambda_{18}}{dt} = -\frac{\partial\mathcal{H}}{\partial I_{VD}},\ \lambda_{18}(t_f)=0$$

Evaluated at the optimal control vector $(u_1(t), u_2(t), u_3(t), u_4(t), u_5(t), u_6(t))$ and corresponding optimal states, which yields the adjoint system [3] and transversality conditions [4].

Considering the optimality conditions:

$$\frac{\partial\mathcal{H}}{\partial u_1}=0, \quad \frac{\partial\mathcal{H}}{\partial u_2}=0, \quad \frac{\partial\mathcal{H}}{\partial u_3}=0, \quad \frac{\partial\mathcal{H}}{\partial u_4}=0, \quad \frac{\partial\mathcal{H}}{\partial u_5}=0, \quad \frac{\partial\mathcal{H}}{\partial u_6}=0$$

To obtain the optimal control $u_1^*(t)$, we have:

$$\begin{aligned}\frac{\partial\mathcal{H}}{\partial u_1} = {} & \frac{I_{VD}S_Hb\beta_D\lambda_2(u_2-1)}{N_H}+\frac{I_{VM}S_Hb\beta_M\lambda_3(u_2-1)}{N_H}\\ & -\Big(\frac{I_{VD}S_Hb\beta_D(u_2-1)}{N_H}+\frac{I_{VM}S_Hb\beta_M(u_2-1)}{N_H}\Big)\lambda_1+A_4u_1=0\end{aligned}$$

$$\Longrightarrow u_1^* = \frac{(I_{VD}S_H b\beta_D + I_{VM}S_H b\beta_M)(\lambda_2 - \lambda_1)(u_2 - 1)}{A_4 N_H}$$

On the set $\{t|0 < u_1^*(t) < 1\}$.

To obtain the optimal control $u_2^*(t)$, we have:

$$\begin{aligned}\frac{\partial \mathcal{H}}{\partial u_2} = &\frac{I_{VD}S_H b\beta_D\lambda_2(u_1-1)}{N_H} + \frac{I_{VM}S_H b\beta_M\lambda_3(u_1-1)}{N_H} \\ &+\frac{(I_{DM}+I_M)S_{VM}\beta_{VM}\lambda_{15}}{N_H} - \frac{(I_{DM}+I_M)S_{VM}\beta_{VM}\lambda_{16}}{N_H} \\ &-\Big(\frac{I_{VD}S_H b\beta_D(u_1-1)}{N_H} + \frac{I_{VM}S_H b\beta_M(u_1-1)}{N_H}\Big)\lambda_1 + A_5 u_2 = 0\end{aligned}$$

$$\Longrightarrow u_2^* = \frac{(I_{VD}S_H b\beta_D + I_{VM}S_H b\beta_M)(\lambda_2 - \lambda_1)(u_1 - 1) + (I_{DM} + I_M)S_{VM}\beta_{VM}(\lambda_{16} - \lambda_{15})}{A_5 N_H}$$

On the set $\{t|0 < u_2^*(t) < 1\}$.

To obtain the optimal control $u_3^*(t)$, we have:

$$\frac{\partial \mathcal{H}}{\partial u_3} = \frac{(I_D+I_{DM})S_{VD}\beta_{VD}\lambda_{17}}{N_H} - \frac{(I_D+I_{DM})S_{VD}\beta_{VD}\lambda_{18}}{N_H} + A_6 u_3 = 0$$

$$\Longrightarrow u_3^* = \frac{(I_D + I_{DM})S_{VD}\beta_{VD}(\lambda_{18} - \lambda_{17})}{A_6 N_H}$$

On the set $\{t|0 < u_3^*(t) < 1\}$.

To obtain the optimal control $u_4^*(t)$, we have:

$$\frac{\partial \mathcal{H}}{\partial u_4} = \frac{E_D I_{VM} b\beta_M\lambda_2}{N_H} + \frac{E_M I_{VD} b\beta_D\lambda_3}{N_H} - \Big(\frac{E_M I_{VD} b\beta_D}{N_H} + \frac{E_D I_{VM} b\beta_M}{N_H}\Big)\lambda_4 + A_7 u_4 = 0$$

$$\Longrightarrow u_4^* = \frac{(E_M I_{VD} b\beta_D + E_D I_{VM} b\beta_M)\Big(\lambda_4 - \frac{E_D\lambda_2 + E_M\lambda_3}{E_D + E_M}\Big)}{A_7 N_H}$$

On the set $\{t|0 < u_4^*(t) < 1\}$.

To obtain the optimal control $u_5^*(t)$, we have:

$$\frac{\partial \mathcal{H}}{\partial u_5} = -I_{DM}\lambda_{10}\phi_2 + I_{DM}\lambda_7\phi_2 + A_8 u_5 = 0$$

$$\Longrightarrow u_5^* = \frac{I_{DM}\phi_2(\lambda_{10} - \lambda_7)}{A_8}$$

On the set $\{t|0 < u_5^*(t) < 1\}$.

To obtain the optimal control $u_6^*(t)$, we have:

$$\frac{\partial \mathcal{H}}{\partial u_6} = -S_H\lambda_1 + S_H\lambda_{11} + A_9u_6 = 0$$

$$\Longrightarrow u_6^* = \frac{S_H(\lambda_1 - \lambda_{11})}{A_9}$$

On the set $\{t|0 < u_6^*(t) < 1\}$.

Solving for u_i^*, $(i = 1, 2, 3, 4, 5, 6)$ considering the state variables and applying the control constraints yields the characterizations presented in [5]. The optimality conditions involving the partial derivatives of the Hamiltonian with respect to each control are valid only within the interior of the admissible control set Υ.

□

4.2. **Numerical simulation of the model with optimal control measures.**

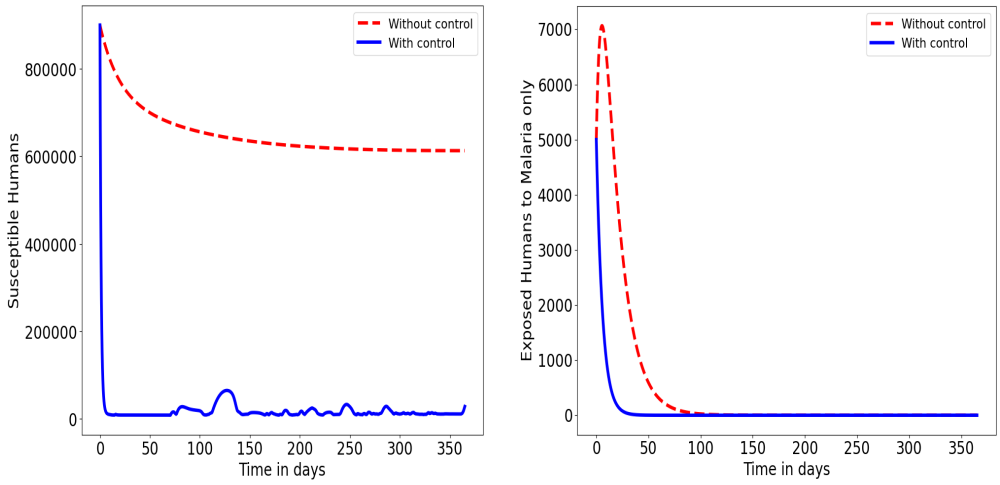

(a) (b)

FIGURE 6. Impact of controls on the susceptible and exposed classes.

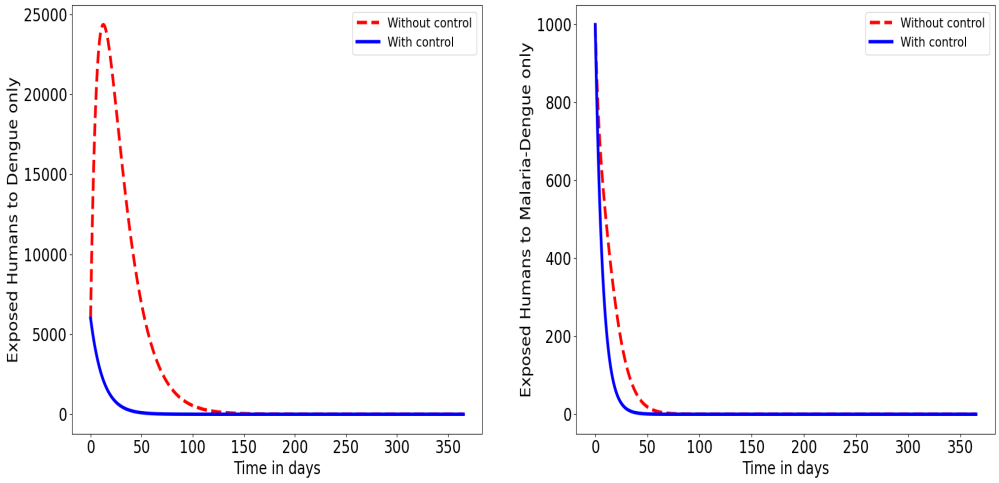

(a) (b)

FIGURE 7. Impact of controls on the exposed classes on dengure and malaria infection.

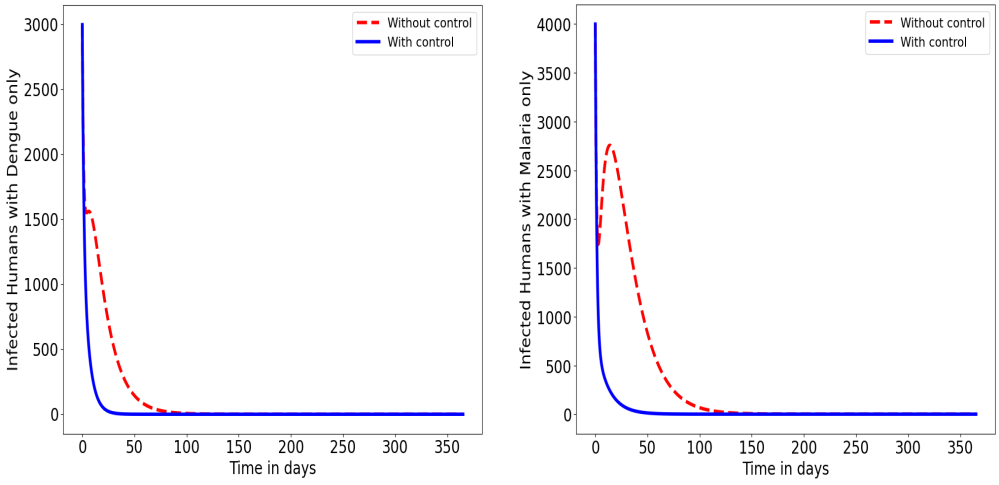

(a) (b)

FIGURE 8. Impact of controls on the infected classes on dengue and malaria infection.

SPECIAL CASES

We proceed further by implementing various combinations of control strategies rather than deploying all six time-dependent control parameters simultaneously in our fundamental model. This approach is undertaken to further reduce the costs related to mitigating the co-dynamics of malaria and dengue fever in the human population.

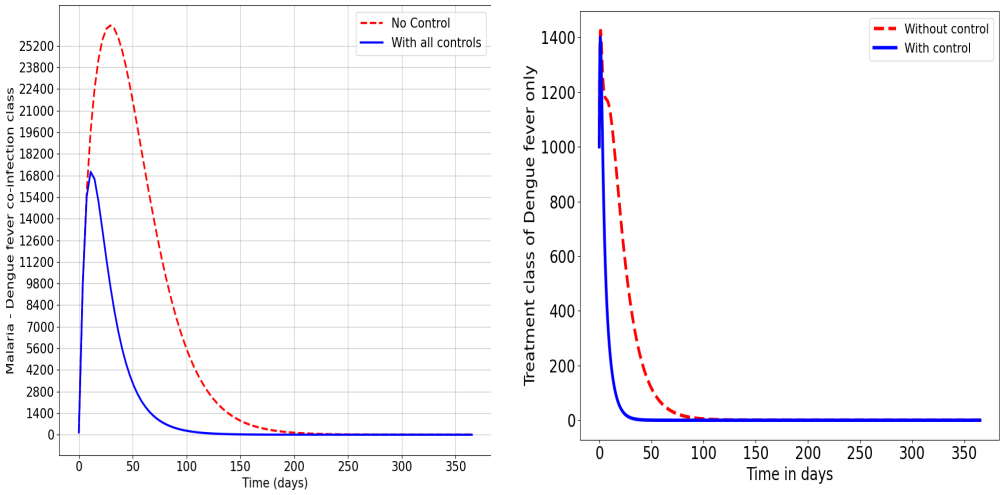

(a) (b)

FIGURE 9. Impact of controls on the co-infection and treatment classes.

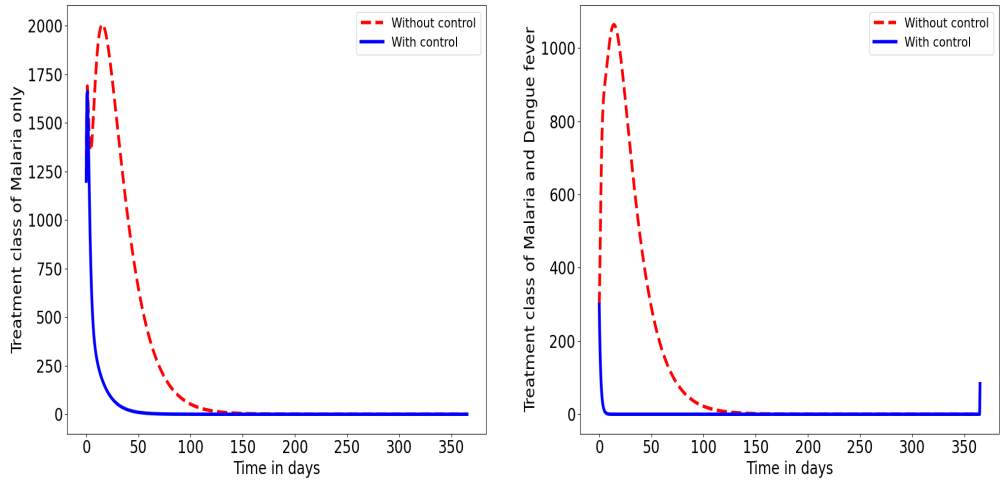

(a) (b)

FIGURE 10. Impact of controls on the treatment classes.

TABLE 6. **Possible Scenarios with their combination strategy**

Scenario	**Strategies**
A	1. $(u_1 \neq 0, u_2 \neq 0)$ 2. $(u_3 \neq 0, u_4 \neq 0)$
B	3. $(u_2 \neq 0, u_3 \neq 0, u_4 \neq 0)$ 4. $(u_1 \neq 0, u_5 \neq 0)$
C	5. $(u_1 \neq 0, u_2 \neq 0, u_3 \neq 0)$ 6. $(u_2 \neq 0, u_4 \neq 0, u_5 \neq 0, u_6 \neq 0)$
D	7. $(u_1 \neq 0, u_2 \neq 0, u_3 \neq 0, u_4 \neq 0, u_5 \neq 0)$ 8. $(u_1 \neq 0, u_2 \neq 0, u_3 \neq 0, u_4 \neq 0, u_6 \neq 0)$
E	9. $(u_1 \neq 0, u_2 \neq 0, u_3 \neq 0, u_4 \neq 0, u_5 \neq 0, u_6 \neq 0)$

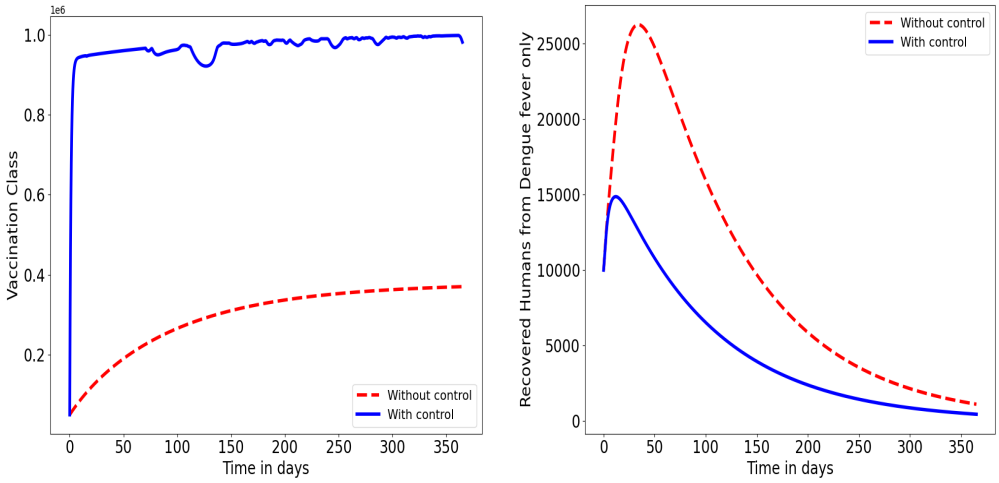

(a) (b)

FIGURE 11. Impact of controls on the vaccination and treatment classes.

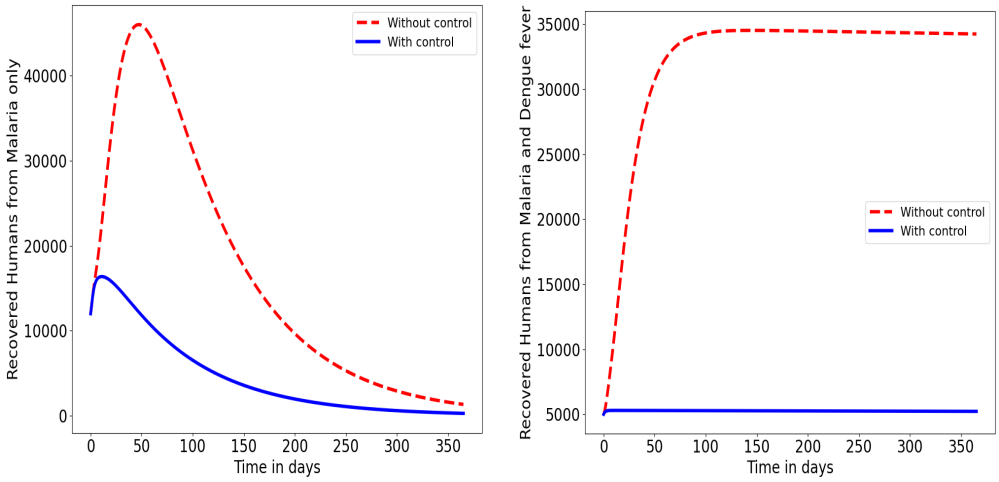

(a) (b)

FIGURE 12. Effect of control measures on the recovered humans from malaria only and co-infection.

Strategy 1: The optimal implementation of insecticide-treated bed nets (ITNs) and indoor residual spraying (IRS) only $(u_1 \neq 0, u_2 \neq 0)$

Figure [15(a)] demonstrates the effectiveness of optimally applying ITNs and IRS in combating the co-infection of malaria and dengue fever within the human population. Observations indicate that following the 360-day period, a cumulative total of 26,000 individuals experienced co-infection with malaria and dengue fever in the absence of these control interventions in

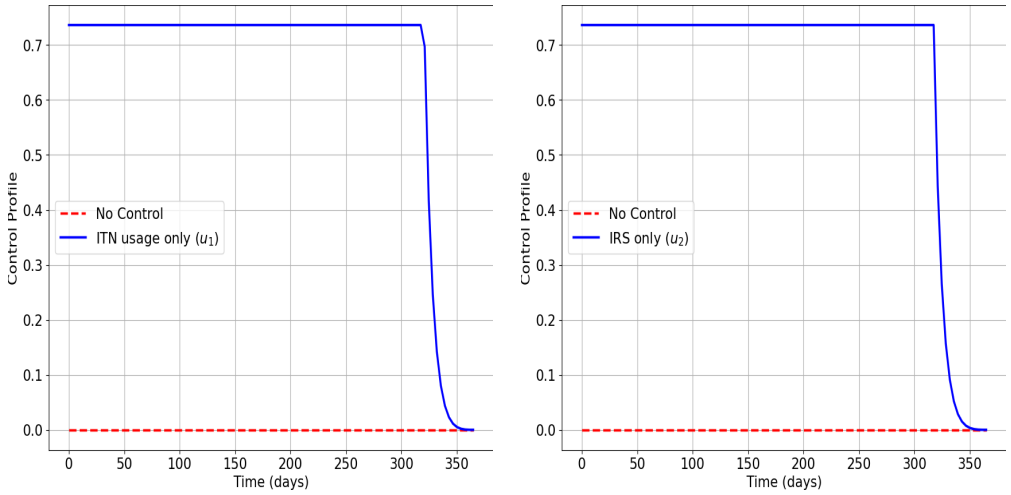

(a) (b)

FIGURE 13. Control Profiles of u_1 and u_2.

strategy 1. Nevertheless, implementing this dual-measure approach resulted in a decrease in the overall number of co-infections to 25,300 individuals, thereby reducing co-infections by 700 cases. This demonstrates a measurable impact in diminishing the disease burden of the co-infection of these two diseases, preventing 2.69% of the total number of co-infection cases.

Strategy 2: The optimal implementation of environmental management and personal protection measures only $(u_3 \neq 0, u_4 \neq 0)$

Figure [15(b)] demonstrates the effectiveness of optimally deploying environmental management combined with personal protection measures to address the co-infection of malaria and dengue fever within the human population. Observations reveal that throughout the 360-day duration, a cumulative total of 26,000 individuals experienced co-infection without the deployment of these control interventions in strategy 2. However, by integrating these two measures, the total co-infection cases declined to 23,500 individuals, yielding a reduction of 2,500 co-infections. This indicates a substantial decrease in the disease burden related to the co-infection of these two diseases, preventing 9.62% of the total co-infection cases.

Strategy 3: The optimal implementation of IRS, environmental management, and personal protection measures $(u_2 \neq 0, u_3 \neq 0, u_4 \neq 0)$

Figure [16(a)] illustrates the effectiveness of optimally implementing IRS, environmental management, and personal protection measures for managing co-infection in the human population. During the 360-day observation period, the absence of control interventions in strategy

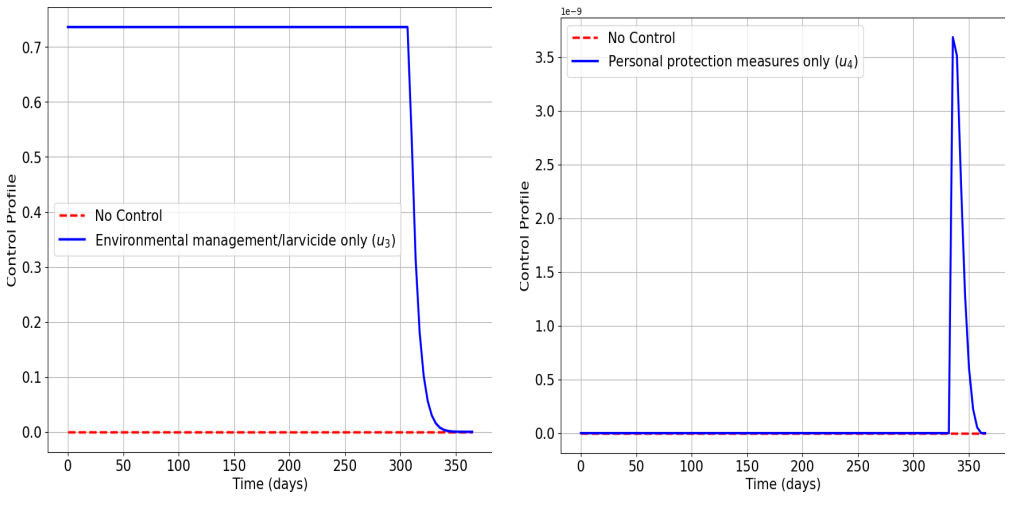

(a) (b)

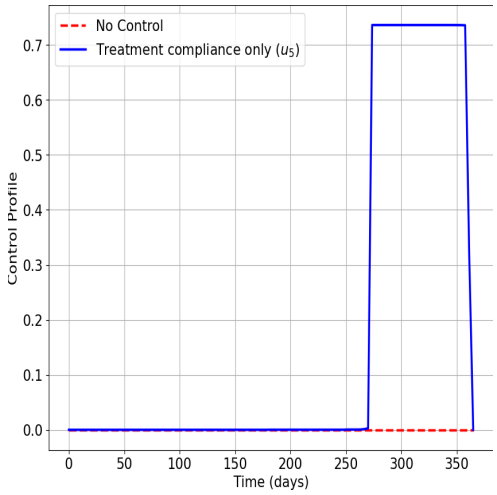

(c)

FIGURE 14. Control Profiles of u_3, u_4 and u_5.

3 resulted in a total of 26,000 individuals experiencing co-infection with malaria and dengue fever. Nevertheless, with the deployment of these three measures, the total co-infection cases reduced to 24,200 individuals, representing a decrease of 1,800 co-infections. This underscores a notable impact in alleviating the disease burden of the co-infection, preventing 6.92% of the total co-infection cases.

Strategy 4: The optimal implementation of ITNs and treatment compliance $(u_1 \neq 0, u_5 \neq 0)$

Figure [16(b)] demonstrates the effectiveness of optimal adherence to the utilization of ITNs and treatment compliance for malaria and dengue fever co-infection within the human

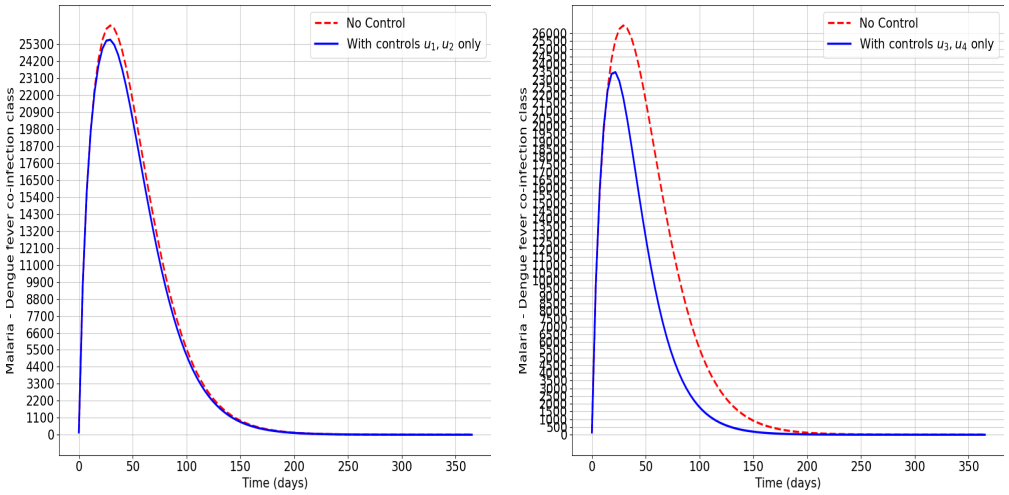

(a) (b)

FIGURE 15. Impact of special cases on the malaria dengue fever co-infection class.

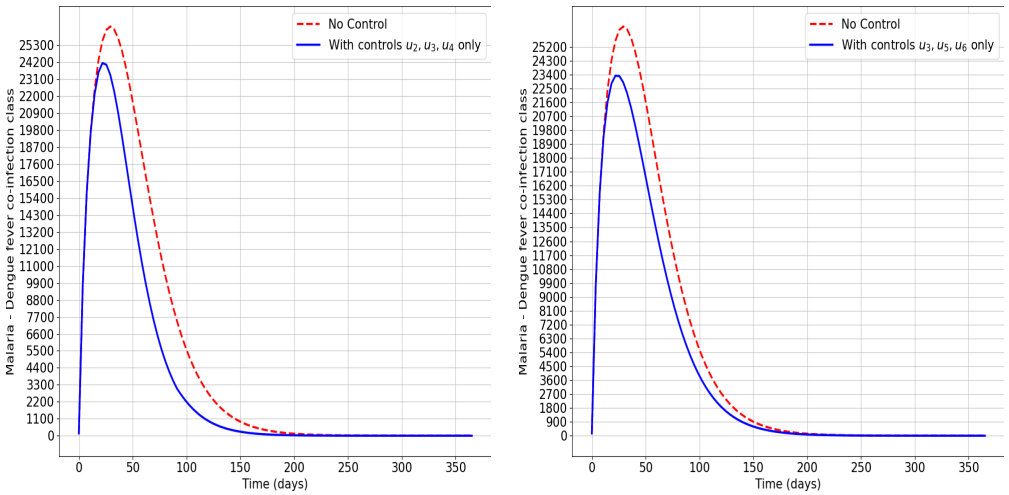

(a) (b)

FIGURE 16. Impact of special cases on the malaria dengue fever co-infection class.

population. Observations indicate that following the 360-day period, a cumulative total of 26,000 individuals experienced co-infections of malaria and dengue fever when these control interventions were not deployed in strategy 4. However, by deploying these two measures, the total co-infection cases decreased to 23,400 individuals, yielding a reduction of 2,600 co-infections. This indicates a considerable decrease in the disease burden of the co-infection,

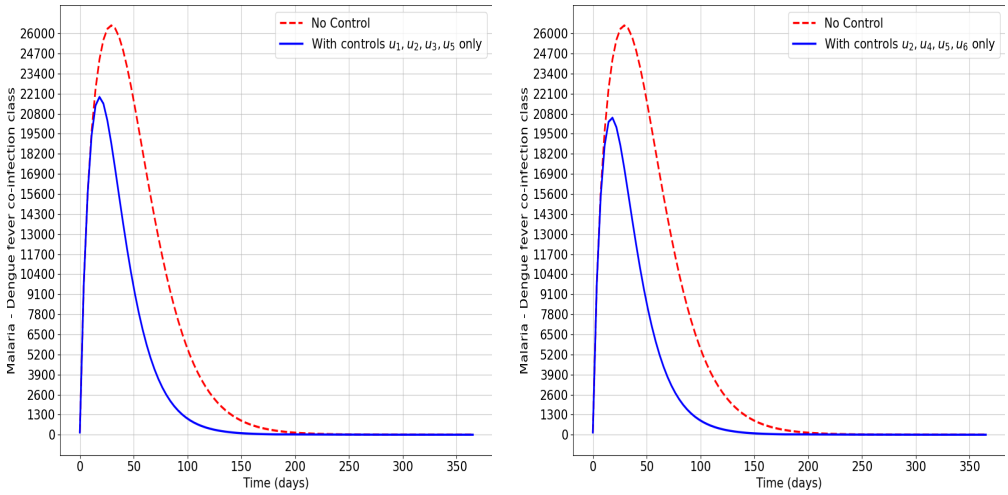

(a) (b)

FIGURE 17. Impact of special cases on the malaria dengue fever co-infection class.

preventing 10.00% of the total co-infection cases.

Strategy 5: The optimal deployment of ITNs, IRS, and environmental management $(u_1 \neq 0, u_2 \neq 0, u_3 \neq 0)$

Figure [17(a)] demonstrates the effectiveness of adhering to the optimal implementation of ITNs, IRS, and environmental management within the human population. Throughout a 360-day duration, without deploying these control interventions in strategy 5, a cumulative total of 26,000 individuals experienced co-infections of malaria and dengue fever. However, by deploying these three measures, the total co-infection cases declined to 22,100 individuals, leading to a reduction of 3,900 co-infections. This indicates a substantial impact in reducing the disease burden of the co-infection, preventing 15.00% of the total co-infection cases.

Strategy 6: The optimal deployment of IRS, personal protection, treatment compliance, and vaccination $(u_2 \neq 0, u_4 \neq 0, u_5 \neq 0, u_6 \neq 0)$

Figure [17(b)] illustrates the effectiveness of adhering to optimal implementation of IRS, personal protection measures, treatment compliance for co-infected individuals, and vaccination within the human population. Throughout the 360-day observation period, it was documented that without deploying these control interventions in strategy 6, a cumulative total of 26,000 individuals experienced co-infections of malaria and dengue fever. However, by deploying these four measures, the overall number of co-infections declined to 20,800 individuals, yielding a

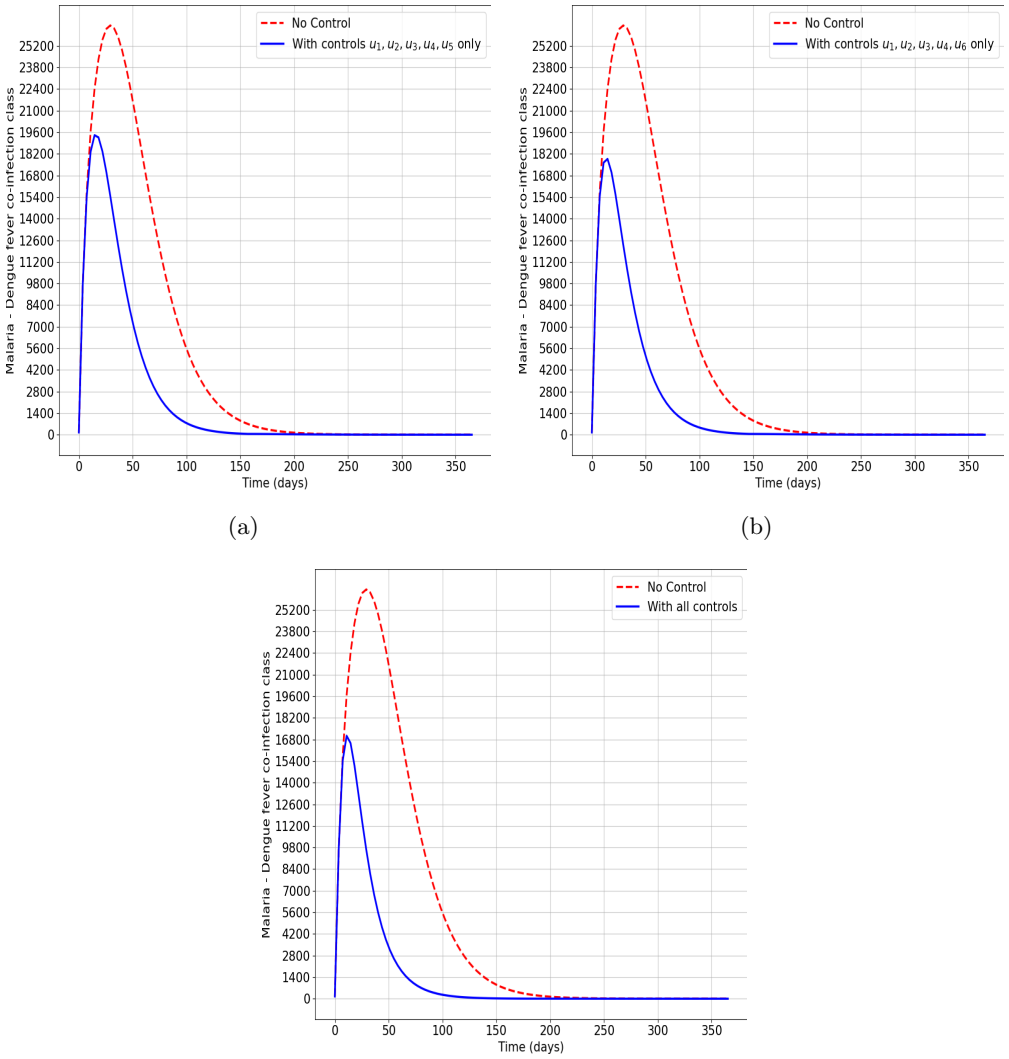

FIGURE 18. Impact of special cases on the malaria dengue fever co-infection class.

reduction of 5,200 co-infections. This indicates a substantial impact on reducing the disease burden of the co-infection, preventing 20.00% of the total number of co-infection cases.

Strategy 7: The optimal deployment of ITNs, IRS, environmental management, personal protection, and treatment compliance $(u_1 \neq 0, u_2 \neq 0, u_3 \neq 0, u_4 \neq 0, u_5 \neq 0)$

Figure [18(a)] depicts the effectiveness of adhering to five control approaches within the human population. Results demonstrate that, following the 360-day duration, a cumulative count of 26,000 individuals experienced co-infection of malaria and dengue fever when strategy 7 lacked control interventions. However, with the deployment of these five measures, the

co-infection total decreased to 19,600 individuals, leading to a reduction of 6,400 co-infections. This indicates a very substantial reduction in the disease burden associated with the co-infection, preventing 24.62% of the overall co-infection cases.

Strategy 8: The optimal deployment of ITNs, IRS, environmental management, personal protection, and vaccination $(u_1 \neq 0, u_2 \neq 0, u_3 \neq 0, u_4 \neq 0, u_6 \neq 0)$

Figure [18(b)] illustrates the effectiveness of adhering to ITNs, IRS, environmental management, personal protection measures, and vaccination within the human population. Throughout the 360-day period, without deploying these control interventions in strategy 8, a cumulative total of 26,000 individuals experienced co-infections. However, by deploying these five measures, the total co-infection cases decreased to 18,200 individuals, yielding a reduction of 7,800 co-infections. This indicates a substantial impact in reducing the disease burden, preventing 30.00% of the total co-infection cases.

Strategy 9: The optimal deployment of all control strategies $(u_1 \neq 0, u_2 \neq 0, u_3 \neq 0, u_4 \neq 0, u_5 \neq 0, u_6 \neq 0)$

Figure [18(c)] depicts the effectiveness of adhering to all six control approaches within the human population. Results demonstrate that, following the 360-day duration, a cumulative count of 26,000 individuals experienced co-infection when strategy 9 lacked control interventions. However, with the deployment of all six measures, the co-infection total decreased to 16,800 individuals, leading to a reduction of 9,200 co-infections. This indicates a substantial reduction in the disease burden, preventing 35.38% of the overall co-infection cases.

4.3. **Cost Effectiveness Analysis in Reducing the Number of Co-infection Cases of Malaria and Dengue Fever.** The well-established costs and severity of disease mitigation are particularly pronounced in densely populated and resource-limited regions. Therefore, it becomes imperative to explore the most economically viable yet readily accessible interventions to reduce the impact of malaria-dengue fever co-infection within a given population. This section employs cost-effectiveness analysis to examine the most economical control strategy from various combinations spanning Scenario A through Scenario E. We utilize three distinct approaches—the infection averted ratio (IAR), average cost-effectiveness ratio (ACER), and incremental cost-effectiveness ratio (ICER)—to accomplish this objective. Subsequent sections elaborate on each methodology and the estimates they yield for the control strategies.

4.3.1. *Infection Averted Ratio (IAR).* The proportion of individuals who have recovered from an infection due to the intervention compared to the number of infections averted by the intervention is termed the infection averted ratio (IAR). This is calculated as

$$\text{IAR} = \frac{\text{Number of infections averted}}{\text{Number of recovered individuals from the infection}}$$

Thus, we obtained the values of IAR for strategies 1-9 as follows:

Scenario A

$$\text{IAR}(1) = \frac{26,000 - 25,300}{5,000} = \frac{700}{5,000} = 0.1400$$

$$\text{IAR}(2) = \frac{26,000 - 23,500}{5,000} = \frac{2,500}{5,000} = 0.5000$$

Scenario B

$$\text{IAR}(3) = \frac{26,000 - 24,200}{5,000} = \frac{1,800}{5,000} = 0.3600$$

$$\text{IAR}(4) = \frac{26,000 - 23,400}{5,000} = \frac{2,600}{5,000} = 0.5200$$

Scenario C

$$\text{IAR}(5) = \frac{26,000 - 22,100}{5,000} = \frac{3,900}{5,000} = 0.7800$$

$$\text{IAR}(6) = \frac{26,000 - 20,800}{5,000} = \frac{5,200}{5,000} = 1.0400$$

Scenario D

$$\text{IAR}(7) = \frac{26,000 - 19,600}{5,000} = \frac{6,400}{5,000} = 1.2800$$

$$\text{IAR}(8) = \frac{26,000 - 18,200}{5,000} = \frac{7,800}{5,000} = 1.5600$$

Scenario E

$$\text{IAR}(9) = \frac{26,000 - 16,800}{5,000} = \frac{9,200}{5,000} = 1.8400$$

It is important to note that the number of infections averted (IA) is determined by comparing the total infectious individuals under optimal control to the total infected individuals under no control. As highlighted in the literature, the method with the highest infection averted ratio is the most economical in halting the spread of diseases among the population. The estimates of the infection averted ratio for the nine strategies considered in this study are presented in Figures [19] and [20], while Figure [21] illustrates the IAR bar plots and infections averted across all strategies.

The IAR analysis reveals that in Scenario A, IAR(2) surpasses IAR(1) as depicted in Figure [19(a)], making strategy 2 the most economically efficient approach to reducing malaria-dengue fever co-infection cases in the human population. Similarly, in Scenario B, IAR(4) surpasses IAR(3) as shown in Figure [19(b)], establishing strategy 4 as the most cost-effective option for Scenario B. Additionally, in Scenario C, IAR(6) exceeds IAR(5) as illustrated in Figure [20(a)], indicating that strategy 6 is the most economical choice for Scenario C. Furthermore, in Scenario D, IAR(8) exceeds IAR(7) as demonstrated in Figure [20(b)], showing that strategy 8 is the most cost-effective option for Scenario D. Consequently, the most cost-effective strategies

across Scenarios A through D are strategies 2, 4, 6, and 8, respectively. The subsequent subsection will evaluate the most cost-effective strategy among those in Scenarios A through E, employing the average cost-effectiveness ratio approach.

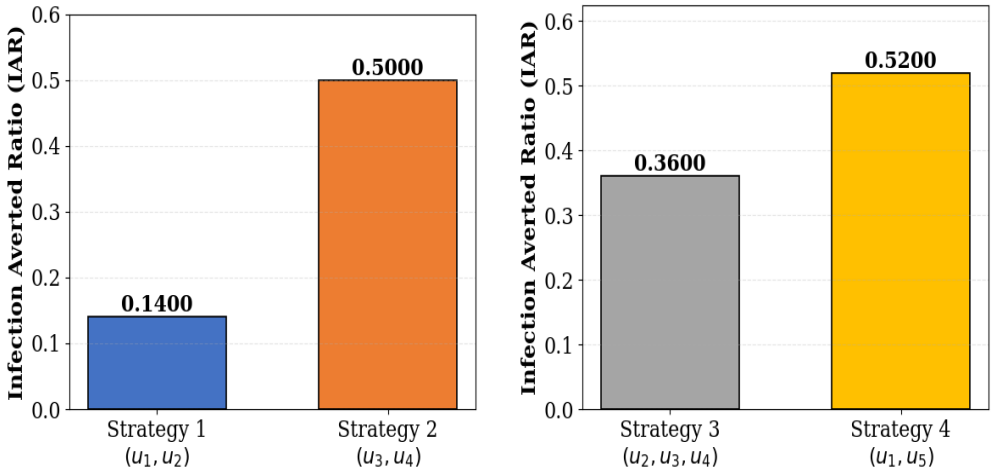

(a) (b)

FIGURE 19. Infection Averted Ratios for Scenarios A and B.

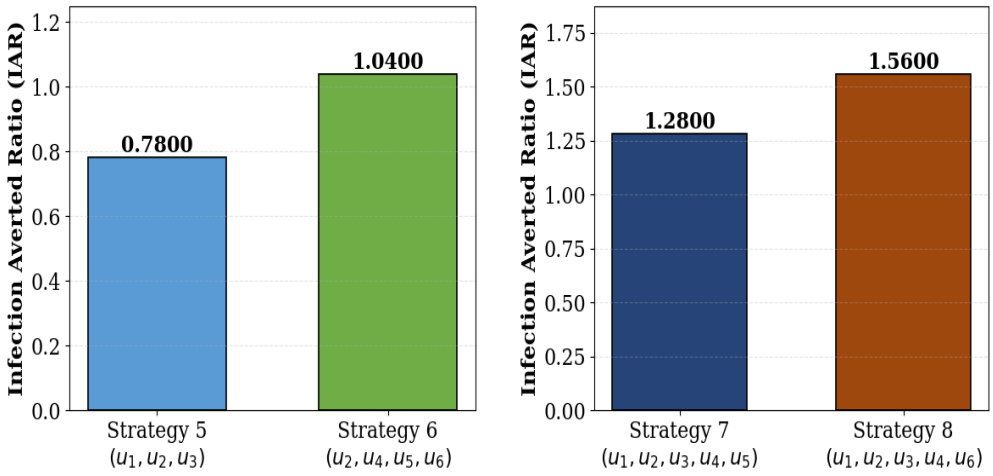

(a) (b)

FIGURE 20. Infection Averted Ratios for Scenarios C and D.

4.4. **Average Cost-Effectiveness Ratio (ACER).** The Average Cost-Effectiveness Ratio (ACER) is defined as the ratio of the total cost of implementing a control strategy to the total number of infections averted by that strategy. It is calculated as:

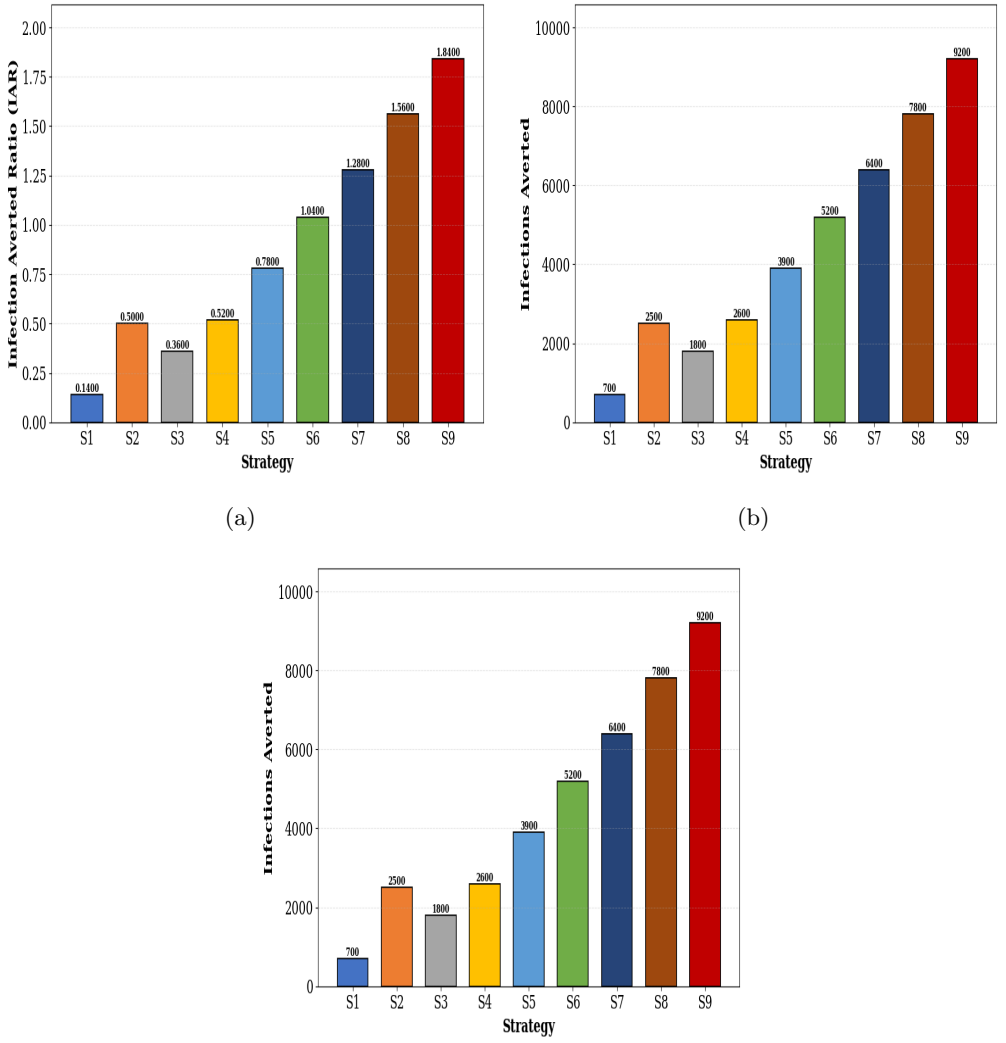

FIGURE 21. Infection Averted Ratios and Infections Averted for All Strategies.

$$\text{ACER} = \frac{\text{Total cost of the strategy}}{\text{Total number of infections averted}}$$

The ACER values for strategies 1-9 are computed as follows:

Scenario A

$$\text{ACER}(1) = \frac{34,560,065.25}{700} = 49,371.522$$

$$\text{ACER}(2) = \frac{34,560,032.4}{2,500} = 13,824.013$$

Scenario B

$$\text{ACER}(3) = \frac{34,560,068.85}{1,800} = 19,200.038$$

$$\text{ACER}(4) = \frac{34,560,050.85}{2,600} = 13,292.327$$

Scenario C

$$\text{ACER}(5) = \frac{34,560,081.45}{3,900} = 8,861.559$$

$$\text{ACER}(6) = \frac{34,560,085.95}{5,200} = 6,646.170$$

Scenario D

$$\text{ACER}(7) = \frac{34,560,119.7}{6,400} = 5,400.019$$

$$\text{ACER}(8) = \frac{34,560,108.9}{7,800} = 4,430.783$$

Scenario E

$$\text{ACER}(9) = \frac{34,560,130.95}{9,200} = 3,756.536$$

The ACER values for Scenarios A and B are depicted in Figure [22], while those for Scenarios C and D are presented in Figure [23]. The overall comparison across all strategies is illustrated in Figure [24]. The ACER analysis indicates that Strategy 9 (all six controls) has the lowest ACER value of 3,756.536, making it the most cost-effective strategy overall. Within each scenario, the most cost-effective strategies based on ACER are: Strategy 2 for Scenario A (ACER = 13,824.013) as shown in Figure [22(a)], Strategy 4 for Scenario B (ACER = 13,292.327) as depicted in Figure [22(b)], Strategy 6 for Scenario C (ACER = 6,646.170) as illustrated in Figure [23(a)], and Strategy 8 for Scenario D (ACER = 4,430.783) as demonstrated in Figure [23(b)].

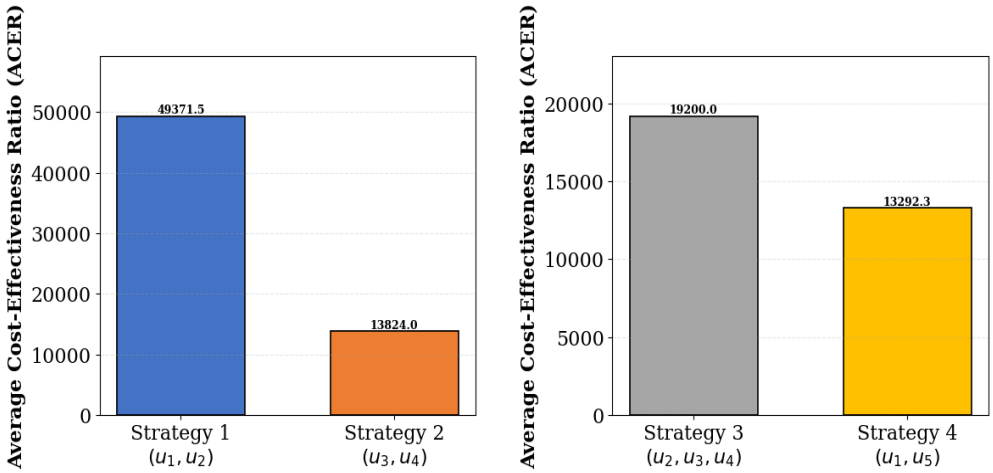

FIGURE 22. Average Cost Effectiveness Ratio for Scenarios A and B.

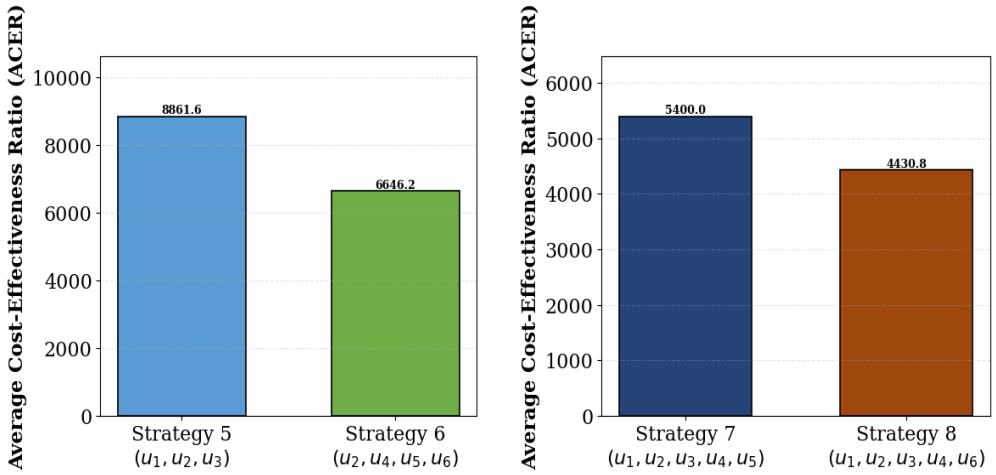

(a) (b)

FIGURE 23. Average Cost Effectiveness Ratio for Scenarios C and D.

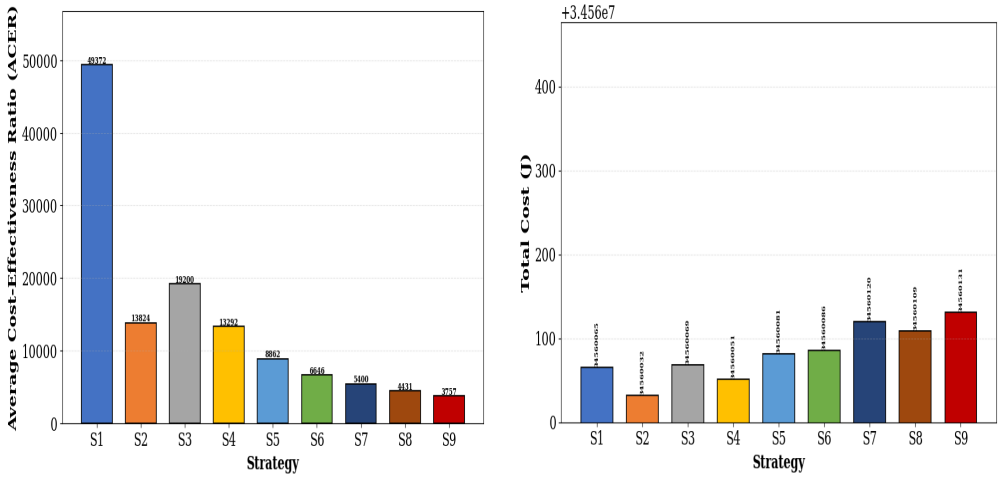

(a) (b)

FIGURE 24. Average Cost Effectiveness Ratio and Total Cost for All Strategies.

4.4.1. *Incremental Cost Effectiveness Ratio (ICER).* In this segment, we explore the most economical tactic among all the approaches in Scenarios A to E employing the incremental cost-effectiveness ratio method. The disparity between two or more rival strategies, considering their related health advantages and implementation expenditures, is ascertained using the ICER. This is computed by

$$\text{ICER} = \frac{\text{Difference in total costs between control strategies}}{\text{Difference in total infections averted by control strategies}}$$

In the sections that follow, we will discuss how to estimate each strategy for its respective scenarios.

Scenario A

We present the co-infection averted, the total cost of implementation, ACER, and ICER in Table [7] in increasing order of the infections averted in order to determine the most cost-effective strategy in Scenario A (strategies 1 and 2). The ICER's derivation is provided as follows:

$$\text{ICER}(1) = \frac{34{,}560{,}065.25}{700} = 49,371.522$$

$$\text{ICER}(2) = \frac{34{,}560{,}032.4 - 34{,}560{,}065.25}{2{,}500 - 700} = \frac{-32.85}{1{,}800} = -0.01825$$

Since ICER(2) is negative, strategy 2 dominates strategy 1 (it costs less and achieves more infections averted). We eliminate strategy 1.

$$\text{ICER}(2) = \frac{34{,}560{,}032.4}{2{,}500} = 13,824.013$$

Therefore, strategy 2 is the most cost-effective strategy in Scenario A.

TABLE 7. **ICER for strategies in Scenario A**

Strategies	Infection Averted	Total Cost	ACER	ICER
2	2,500	34,560,032.4	13,824.013	13,824.013

Scenario B

We present the co-infection averted, the total cost of implementation, ACER, and ICER in Table [8] in increasing order of the infections averted in order to determine the most cost-effective strategy in Scenario B (strategies 3 and 4). The ICER's derivation is provided as follows:

$$\text{ICER}(3) = \frac{34{,}560{,}068.85}{1{,}800} = 19,200.038$$

$$\text{ICER}(4) = \frac{34{,}560{,}050.85 - 34{,}560{,}068.85}{2{,}600 - 1{,}800} = \frac{-18.0}{800} = -0.0225$$

Since ICER(4) is negative, strategy 4 dominates strategy 3 (it costs less and achieves more infections averted). We eliminate strategy 3.

$$\text{ICER}(4) = \frac{34{,}560{,}050.85}{2{,}600} = 13,292.327$$

Therefore, strategy 4 is the most cost-effective strategy in Scenario B.

TABLE 8. **ICER for strategies in Scenario B**

Strategies	Infection Averted	Total Cost	ACER	ICER
4	2,600	34,560,050.85	13,292.327	13,292.327

Scenario C

We present the co-infection averted, the total cost of implementation, ACER, and ICER in Table [9] in increasing order of the infections averted in order to determine the most cost-effective strategy in Scenario C (strategies 5 and 6). The ICER's derivation is provided as follows:

$$\text{ICER}(5) = \frac{34{,}560{,}081.45}{3{,}900} = 8,861.559$$

$$\text{ICER}(6) = \frac{34{,}560{,}085.95 - 34{,}560{,}081.45}{5{,}200 - 3{,}900} = \frac{4.5}{1{,}300} = 0.003462$$

Since ICER(6) < ICER(5), strategy 6 is the most cost-effective strategy in Scenario C.

TABLE 9. **ICER for strategies in Scenario C**

Strategies	Infection Averted	Total Cost	ACER	ICER
5	3,900	34,560,081.45	8,861.559	8,861.559
6	5,200	34,560,085.95	6,646.170	0.003462

Scenario D

We present the co-infection averted, the total cost of implementation, ACER, and ICER in Table [10] in increasing order of the infections averted in order to determine the most cost-effective strategy in Scenario D (strategies 7 and 8). The ICER's derivation is provided as follows:

$$\text{ICER}(7) = \frac{34{,}560{,}119.7}{6{,}400} = 5,400.019$$

$$\text{ICER}(8) = \frac{34{,}560{,}108.9 - 34{,}560{,}119.7}{7{,}800 - 6{,}400} = \frac{-10.8}{1{,}400} = -0.007714$$

Since ICER(8) is negative, strategy 8 dominates strategy 7 (it costs less and achieves more infections averted). We eliminate strategy 7.

$$\text{ICER}(8) = \frac{34{,}560{,}108.9}{7{,}800} = 4,430.783$$

Therefore, strategy 8 is the most cost-effective strategy in Scenario D.

TABLE 10. **ICER for strategies in Scenario D**

Strategies	Infection Averted	Total Cost	ACER	ICER
8	7,800	34,560,108.9	4,430.783	4,430.783

The most cost-effective strategy from all scenarios

Now we select strategies 2, 4, and 6 (chosen from Scenarios A, B, and C respectively), along with strategy 8 (from Scenario D) and strategy 9 (Scenario E: all six controls) to analyze the overall minimum-cost strategy among all the techniques in this study. Table [11] presents the infections averted, implementation costs, ACER, and ICER arranged in increasing order of infections averted.

$$\text{ICER}(2) = \frac{34{,}560{,}032.4}{2{,}500} = 13,824.013$$

$$\text{ICER}(4) = \frac{34{,}560{,}050.85 - 34{,}560{,}032.4}{2{,}600 - 2{,}500} = \frac{18.45}{100} = 0.1845$$

$$\text{ICER}(6) = \frac{34{,}560{,}085.95 - 34{,}560{,}050.85}{5{,}200 - 2{,}600} = \frac{35.1}{2{,}600} = 0.0135$$

$$\text{ICER}(8) = \frac{34{,}560{,}108.9 - 34{,}560{,}085.95}{7{,}800 - 5{,}200} = \frac{22.95}{2{,}600} = 0.008827$$

$$\text{ICER}(9) = \frac{34{,}560{,}130.95 - 34{,}560{,}108.9}{9{,}200 - 7{,}800} = \frac{22.05}{1{,}400} = 0.015750$$

All ICER values are positive; hence no further domination exists among the competing strategies.

TABLE 11. **ICER for strategies 2, 4, 6, 8, and 9**

Strategies	Infection Averted	Total Cost	ACER	ICER
2	2,500	34,560,032.4	13,824.013	13,824.013
4	2,600	34,560,050.85	13,292.327	0.1845
6	5,200	34,560,085.95	6,646.170	0.0135
8	7,800	34,560,108.9	4,430.783	0.008827
9	9,200	34,560,130.95	3,756.536	0.015750

From Table [11], we compare strategies 2, 4, 6, 8, and 9. Strategy 9 averts the greatest number of infections (9,200) and carries the lowest ACER (3,756.536) among all competing strategies. Although ICER(8) = 0.008827 is the smallest incremental value, the transition from strategy 8 to strategy 9 yields an acceptable ICER of 0.015750, indicating that the additional expenditure required to deploy all six control measures is justified by the substantial gain of 1,400 additional infections averted. Therefore, among all strategies considered in this study, the combined implementation of ITNs, IRS, environmental management, personal protection, treatment compliance, and vaccination (strategy 9: $u_1 \neq 0, u_2 \neq 0, u_3 \neq 0, u_4 \neq 0, u_5 \neq 0, u_6 \neq 0$) is considered the most cost-effective strategy in reducing the co-infection of malaria and dengue fever cases in the human population.

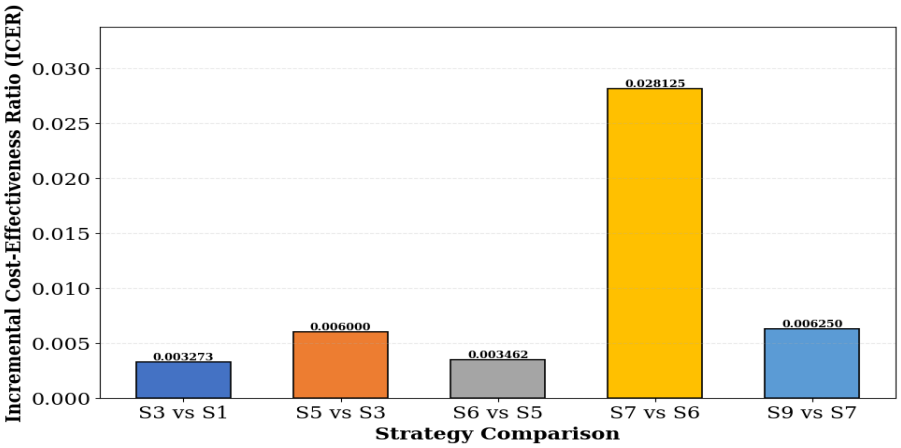

FIGURE 25. **ICER Analysis for Non-Dominated Strategies**

5. CONCLUSION

This study developed a comprehensive mathematical model for malaria-dengue co-infection that explicitly incorporates separate vector populations, disease-specific compartments, and co-infection dynamics. Rigorous mathematical analysis established the model's well-posedness, with basic reproduction numbers derived for both diseases. Model calibration using Brazilian

surveillance data (2011-2023) enabled realistic parameter estimation, though negative R^2 values indicate challenges in capturing epidemic dynamics without enhanced seasonality or serotype structure.

Optimal control analysis of six intervention strategies revealed that integrated approaches substantially reduce disease burden. Sensitivity analysis identified transmission probabilities (β_{VD}, β_{VM}), recruitment rates (π_D, π_M), and progression rates (ε_1, ε_2, ε_3) as critical parameters. Cost-effectiveness analysis using IAR, ACER, and ICER methodologies demonstrated that Strategy 9 (combined ITNs, IRS, environmental management, personal protection, treatment compliance, and vaccination) achieves optimal cost-effectiveness with an ACER of 3,756.536 and ICER of 0.015750, preventing 35.38% of co-infections.

5.1. **Recommendations and Future Research Directions. We make the following recommendations to healthcare policymakers based on our findings from this research work:**

- Measures should be taken to ensure widespread distribution and consistent utilization of insecticide-treated bed nets (ITNs) in malaria-endemic regions, particularly targeting vulnerable populations including pregnant women, children under five, and individuals in co-endemic areas who face elevated risks from both malaria and dengue infections.
- Indoor residual spraying (IRS) programs should be strengthened and sustained for malaria vector control, with particular attention to coverage in high-transmission areas, selection of appropriate insecticides based on local *Anopheles* mosquito resistance patterns, and community engagement to ensure acceptance of interventions.
- Environmental management and larvicide application programs should be prioritized for dengue vector control, focusing on elimination of *Aedes* mosquito breeding sites through community-based source reduction activities, proper waste management, and regular application of larvicides in high-risk areas.

Author's Contributions: Francis Agono: Writing – original draft, Methodology. **Godwin Onuche Acheneje:** Methodology, Formal analysis. **Agbata Benedict Celestine:** Software analysis & editing. **A.K. Awasthi:** Formal analysis. **Hambeer Singh:** Formal analysis. **Aseel Smerat:** Methodology. **Manivel. M:** Formal analysis, Methodology, & editing. **Bolarinwa Bolaj:** Formal analysis & editing.

Competing interests: The authors declare that there is no conflict of interest regarding the publication of this paper.

References

[1] World Health Organization, World Malaria Report 2023, World Health Organization, 2023. https://www.who.int/publications/i/item/9789240086173.

[2] S. Bhatt, D.J. Weiss, E. Cameron, D. Bisanzio, B. Mappin, U. Dalrymple, K.E. Battle, C.L. Moyes, A. Henry, P.A. Eckhoff, E.A. Wenger, O. Briët, M.A. Penny, T.A. Smith, A. Bennett, J. Yukich, T.P. Eisele, J.T. Griffin, C.A. Fergus, M. Lynch, F. Lindgren, J.M. Cohen, C.L.J. Murray, D.L. Smith, S.I. Hay, R.E. Cibulskis, P.W. Gething, The Effect of Malaria Control on Plasmodium falciparum in Africa between 2000 and 2015, Nature 526 (2015), 207–211. https://doi.org/10.1038/nature15535.

[3] S. Bhatt, P.W. Gething, O.J. Brady, J.P. Messina, A.W. Farlow, C.L. Moyes, J.M. Drake, J.S. Brownstein, A.G. Hoen, O. Sankoh, M.F. Myers, D.B. George, T. Jaenisch, G.R.W. Wint, C.P. Simmons, T.W. Scott, J.J. Farrar, S.I. Hay, The Global Distribution and Burden of Dengue, Nature 496 (2013), 504–507. https://doi.org/10.1038/nature12060.

[4] M.G. Guzman, S.B. Halstead, H. Artsob, P. Buchy, J. Farrar, D.J. Gubler, E. Hunsperger, A. Kroeger, H.S. Margolis, E. Martínez, M.B. Nathan, J.L. Pelegrino, C. Simmons, S. Yoksan, R.W. Peeling, Dengue: a Continuing Global Threat, Nat. Rev. Microbiol. 8 (2010), S7–S16. https://doi.org/10.1038/nrmicro2460.

[5] B. Carme, S. Matheus, G. Donutil, O. Raulin, M. Nacher, J. Morvan, Concurrent Dengue and Malaria in Cayenne Hospital, French Guiana, Emerg. Infect. Dis. 15 (2009), 668–671. https://doi.org/10.3201/eid1504.080891.

[6] L. Epelboin, M. Hanf, P. Dussart, S. Ouar-Epelboin, F. Djossou, M. Nacher, B. Carme, Is Dengue and Malaria Co-infection More Severe than Single Infections? A Retrospective Matched-pair Study in French Guiana, Malar. J. 11 (2012), 142. https://doi.org/10.1186/1475-2875-11-142.

[7] R.N. Charrel, P. Brouqui, C. Foucault, X. de Lamballerie, Concurrent Dengue and Malaria, Emerg. Infect. Dis. 11 (2005), 1153–1154. https://doi.org/10.3201/eid1107.041352.

[8] M. Kotepui, K.U. Kotepui, G.D.J. Milanez, F.R. Masangkay, Prevalence of and Risk Factors for Severe Malaria Caused by Plasmodium and Dengue Virus Co-infection: a Systematic Review and Meta-analysis, Infect. Dis. Poverty 9 (2020), 134. https://doi.org/10.1186/s40249-020-00741-z.

[9] G.O. Acheneje, D. Omale, W. Atokolo, B. Bolaji, Modeling the Transmission Dynamics of the Co-infection of COVID-19 and Monkeypox Diseases with Optimal Control Strategies and Cost–Benefit Analysis, Franklin Open 8 (2024), 100130. https://doi.org/10.1016/j.fraope.2024.100130.

[10] B.I. Omede, O.J. Peter, W. Atokolo, B. Bolaji, T.A. Ayoola, A Mathematical Analysis of the Two-Strain Tuberculosis Model Dynamics with Exogenous Re-Infection, Healthc. Anal. 4 (2023), 100266. https://doi.org/10.1016/j.health.2023.100266.

[11] R.M. Anderson, R.M. May, Infectious Diseases of Humans, Oxford University Press, 1991. https://doi.org/10.1093/oso/9780198545996.001.0001.

[12] D.L. Smith, K.E. Battle, S.I. Hay, C.M. Barker, T.W. Scott, F.E. McKenzie, Ross, Macdonald, and a Theory for the Dynamics and Control of Mosquito-Transmitted Pathogens, PLoS Pathog. 8 (2012), e1002588. https://doi.org/10.1371/journal.ppat.1002588.

[13] N.M. Ferguson, C.A. Donnelly, R.M. Anderson, Transmission Dynamics and Epidemiology of Dengue: Insights from Age-Stratified Sero-Prevalence Surveys, Philos. Trans. R. Soc. B Biol. Sci. 354 (1999), 757–768. https://doi.org/10.1098/rstb.1999.0428.

[14] S. Lenhart, J.T. Workman, Optimal Control Applied to Biological Models, Chapman and Hall/CRC, 2007. https://doi.org/10.1201/9781420011418.

[15] S. Olaniyi, O.S. Obabiyi, Qualitative Analysis of Malaria Dynamics with Nonlinear Incidence Function, Appl. Math. Sci. 8 (2014), 3889–3904. https://doi.org/10.12988/ams.2014.45326.

[16] K.O. Okosun, R. Ouifki, N. Marcus, Optimal Control Analysis of a Malaria Disease Transmission Model That Includes Treatment and Vaccination with Waning Immunity, Biosystems 106 (2011), 136–145. https://doi.org/10.1016/j.biosystems.2011.07.006.

[17] L.S. Sepulveda-Salcedo, O. Vasilieva, M. Svinin, Optimal Control of Dengue Epidemic Outbreaks under Limited Resources, Stud. Appl. Math. 144 (2020), 185–212. https://doi.org/10.1111/sapm.12295.

[18] A. Omame, M.E. Isah, M. Abbas, An Optimal Control Model for COVID-19, Zika, Dengue, and Chikungunya Co-Dynamics with Reinfection, Optim. Control Appl. Methods 44 (2022), 170–204. https://doi.org/10.1002/oca.2936.

[19] S.Y. Tchoumi, M.L. Diagne, H. Rwezaura, J.M. Tchuenche, Malaria and COVID-19 Co-Dynamics: A Mathematical Model and Optimal Control, Appl. Math. Model. 99 (2021), 294–327. https://doi.org/10.1016/j.apm.2021.06.016.

[20] K.G. Mekonen, T.G. Habtemicheal, S.F. Balcha, Modeling the Effect of Contaminated Objects for the Transmission Dynamics of COVID-19 Pandemic with Self Protection Behavior Changes, Results Appl. Math. 9 (2021), 100134. https://doi.org/10.1016/j.rinam.2020.100134.

[21] Z. Mukandavire, A.B. Gumel, W. Garira, J.M. Tchuenche, Mathematical Analysis of a Model for HIV-Malaria Co-infection, Math. Biosci. Eng. 6 (2009), 333–362. https://doi.org/10.3934/mbe.2009.6.333.

[22] K. Barley, D. Murillo, S. Roudenko, A.M. Tameru, S. Tatum, A Mathematical Model of HIV and Malaria Co-Infection in Sub-Saharan Africa, J. AIDS Clin. Res. 3 (2012), 173. https://doi.org/10.4172/2155-6113.1000173.